Contributions to the geological mapping of Mors, Denmark – A study based on a large-scale TEM survey

FLEMMING JØRGENSEN, PETER B. E. SANDERSEN, ESBEN AUKEN, HOLGER LYKKE-ANDERSEN & KURT SØRENSEN

DGF

Recent improvements of the transient electromagnetic (TEM) method provide unprecedented capabilities of imaging geological features in the uppermost few hundred metres of the subsurface. This is documented with an example from the island of Mors, Northern Jutland, Denmark, where 2655 TEM soundings have been acquired as a part of Viborg County's hydrogeological investigation programme. Horizontal aspects of the interpreted TEM soundings are presented in thematic maps revealing variations of resistivities in specified depth intervals and depths to the resistivity basement, i.e. the deepest recorded low-resistive layer. Vertical aspects are displayed in cross-sections. The dense coverage of TEM soundings, combined with borehole logs, allows the precise delineation of major geological features. These comprise the Mors salt diapir, intricate systems of buried Quaternary valleys and several glaciotectonic complexes, all contributing to a complicated geological framework for the island. The layers above the salt diapir, which have been subject to severe erosion, are distinctly imaged in the thematic maps, even though they are frequently dissected by buried valleys. At least four generations of buried valleys can be identified on the basis of their preferred orientations; these were mainly formed during early glaciations. Large parts of the island were glaciotectonically deformed during the Late Weichselian subsequent to valley formation, and it is suggested that the presence of deep valleys may have affected the process of glaciotectonic deformation.

Keywords: Transient electromagnetic; TEM; hydrogeophysics; salt diapirs; buried valleys; glaciotectonic deformation; subglacial; Quaternary; Pleistocene; Mors; Denmark.

Flemming Jørgensen [fj@vejleamt.dk], Vejle Amt, Damhaven 12, DK-7100 Vejle, Denmark. Peter B.E. Sandersen [psa@watertech.dk], Watertech a/s, Søndergade 53, DK-8000 Aarhus C, Denmark. Esben Auken [esben.auken@geo.au.dk], Hydrogeophysics Group, Department of Earth Sciences, University of Aarhus, DK-8200 Aarhus N, Denmark. Holger Lykke-Andersen [hla@geo.au.dk], Department of Earth Sciences, University of Aarhus, DK-8200 Aarhus N, Denmark. Kurt Sørensen [kurt.sorensen@geo.au.dk], Hydrogeophysics Group, Department of Earth Sciences, University of Aarhus, DK-8200 Aarhus N, Denmark.

In order to outline aquifers and the vulnerability of water resources, large areas of Denmark have been covered by TEM (Transient ElectroMagnetic) surveys since the early 1990s. During this time the TEM method has undergone, and is still undergoing, intense development as a tool for hydrogeological investigations. This development has primarily taken place within three main areas: 1) technical development (e.g. Danielsen *et al*. 2003; Sørensen & Auken 2004; Sørensen *et al*. 2004a), 2) advances in the handling, modelling and presentation of data (e.g. Effersø *et al*. 1999; GeoFysikSamarbejdet 2003; Auken & Christiansen 2004), and 3) advances in the geological in-terpretation of modelled data (e.g. Poulsen & Christensen 1999; GeoFysikSamarbejdet 2003; Jørgensen *et al*. 2003a, 2003b). The quality of the collected data has also been considerably improved in recent years. Optimized handling of instruments, deletion of noise-infected and coupled soundings and the identification of defective instruments have led to significant improvements of survey results. Experience shows that surveys of large areas with dense data coverage provide a solid base for the construction of geological models.

Traditionally, TEM surveys carried out as part of the Danish counties' hydrogeological investigations
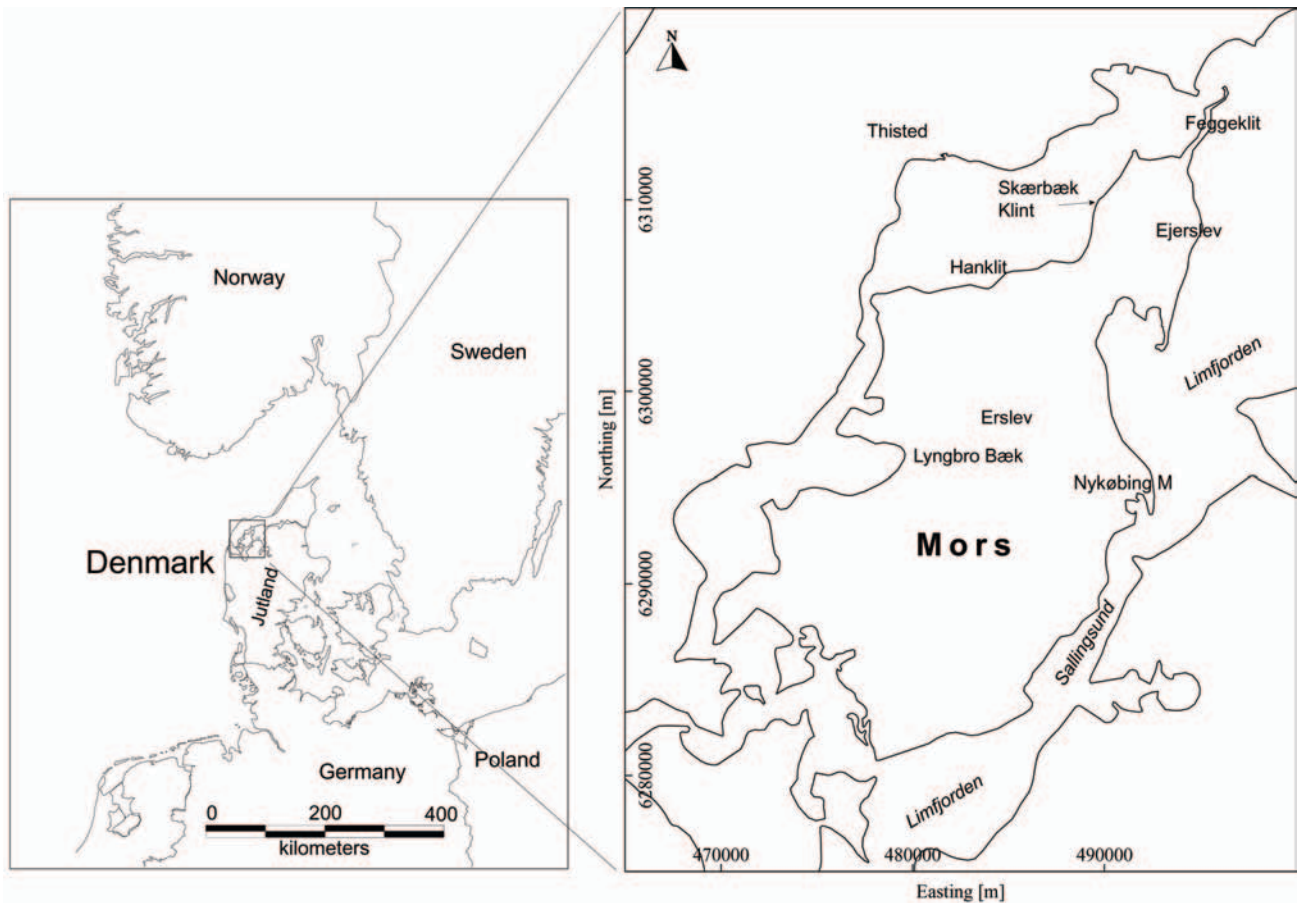
Fig. 1. Location map.

have not been subjected to detailed geological interpretation and have generally not contributed to research in, for example, sedimentology and tertiary and Quaternary geology. The on-going refinements of the TEM methods are, however, expected to lead to significant contributions in above-mentioned fields of research topics. Here we demonstrate how a large-scale TEM survey can be used as the basis for geological interpretation. We show that various types of geological structures can be defined and outlined, and that the understanding and knowledge of near-surface geology can be significantly improved by a detailed study of TEM data. The aim of the paper is two-fold: to demonstrate to what extent TEM data can be used in geological interpretations and to add new information to the geology of Mors.

The geology of Mors is spectacular in several respects: Large-scale glaciotectonic complexes are present in the northern part of the island; the Mors salt diapir is located in the central area; and numerous buried valleys incise the subsurface of the island. These geological elements have previously been described by several authors (e.g. Gry 1940, 1979; El-

sam & Elkraft 1981; Larsen & Baumann 1982; Klint & Pedersen 1995; Pedersen 1996, 2000; Korsager 2002; Jørgensen & Sandersen 2004), who have mainly focused on the individual elements and not on the relations between them.

Study area - the island of Mors
Geography

The study area is confined to the island of Mors, which is situated in the northwestern part of Jutland, Denmark (Fig. 1). The island covers an area of about 360 km². It is 10–15 km wide and about 35 km long with a SSW–NNE trend. The landscape is slightly undulating and mainly dominated by small hills, shallow erosional channels and valleys (Fig. 2). In two areas the terrain reaches altitudes of more than 50 m above sea level (m a.s.l.): In the northwest where parallel ridges reach the highest point (88 m a.s.l.), and in the central southern part where a local upland reaches 66 m a.s.l.
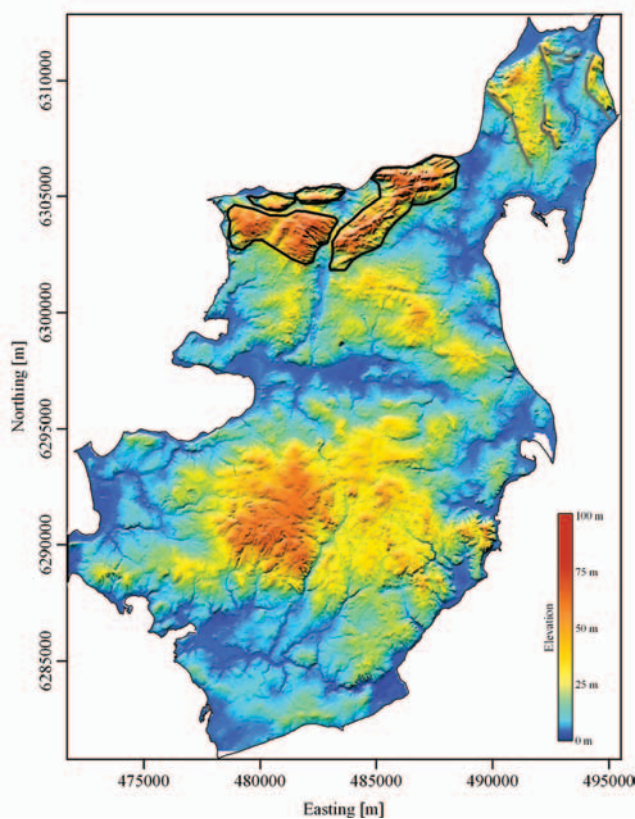
Fig. 2. The topography of Mors. Landscapes in the Hanklit area characterized by composite-ridge systems are marked with black polygons. Grey lines mark ice-marginal moraines in the northeastern part of the island. Scale: 5 km between axis ticks. Coordinate system: UTM zone 32/ED50 (from Viborg Amt with data from National Survey and Cadastre).

Geological setting of Mors

The sub-Quaternary strata comprise Upper Cretaceous white chalk (Maastrichtian) and Paleocene limestone (Danian) covered by clays and diatomite (Paleocene–Eocene). The diatomite is comprised in the Fur Formation (Pedersen & Surlyk 1983). These layers are followed by Oligocene micaceous clay and, to the south, also by Miocene clay, silt and sand (Gravesen 1990, 1993). The Paleogene sediments are in general 50–250 m thick, but locally they are thinner or even absent. They have commonly been subjected to deformation during the Quaternary glaciations, but the most pronounced impact on the Paleogene topography is by a series of incised Quaternary valleys. These valleys have mainly been filled with thick sequences of glacial deposits. Where no valleys exist, only relatively thin layers of glacial origin cover the pre-Quaternary formations.

The overall structure of the tertiary and Quaternary formations on Mors is mainly controlled by 1) the Mors salt diapir, 2) glaciotectonic deformation during the Quaternary glaciations and 3) extensive systems of incised buried valleys.

Halokinetic movements

The Mors salt diapir is located in the central part of the island (Elsam & Elkraft 1981; Larsen & Baumann 1982). The diapir, which is elliptical in shape, covers an area of about 75 km^2 with its long axis trending E-W. Upper Cretaceous white chalk and Danian limestone, together with Paleogene clay and diatomite are uplifted over the salt diapir and along its flanks as a result of halokinetic movements. The top of the Zechstein salt is situated at a depth of more than 400–500 m (Madirazza 1977; Elsam & Elkraft 1981). Erosion has removed some of the pre-Quaternary deposits over the central parts of the diapir so that Quaternary sediments cover the Upper Cretaceous white chalk here. Away from the diapir the chalk is flanked by dipping layers of Danian limestone, followed by Paleogene diatomite and clay. This structural setting is evident in seismic sections (Elsam & Elkraft 1981; Larsen & Baumann 1982), in many boreholes that penetrate the central part as well as the flanks of the diapir (Gravesen 1990, 1993), and in several exposures (Andersen & Sjørring 1992). Pedersen (2000) describes glaciotectonic deformation of Paleogene clay and diatomite on the northern flank of the structure. These deposits are here found at shallow depths as a result of the uplift by the salt diapir.

Glaciotectonic deformation

Significant parts of the island have been affected by glaciotectonic deformation. The most prominent example is the Hanklit glaciotectonic complex in the northwestern part of the island (Fig. 2), where it is exposed in the cliff of Hanklit (Gry 1940; Klint & Pedersen 1995). The system exposed in Hanklit is classified as a large composite-ridge system (Aber *et al.* 1989). More than 50 m thick thrust sheets of Paleogene clay and diatomite that are imbricated into thrust fault complexes are clearly seen in the terrain as several parallel arc-shaped ridges (Fig. 2). A southward moving glacier (the Main Advance, e.g. Kjær *et al.* 2003) is believed to have formed the complex during a Late Weichselian stage (Gry 1940; Klint & Pedersen 1995). The ice movement direction subsequently shifted towards SW and W, and at least three other glaciotectonic deformation complexes were formed in the northeastern part of the island (Gry 1940, 1979; Pedersen 1996, 2000). These complexes are less significantly topographically expressed than

the Hanklit glaciotectonic complex, but some of them form parallel ice-push ridges or elongated ice-shoved hills (Fig. 2). The Paleogene diatomite is commonly found in boreholes and exposures in the area, but always in connection with the glaciotectonic complexes (Gry 1979). The layers of diatomite are thrusted or folded, and they are normally mixed with other tertiary and glacial deposits.

Subglacial erosion

Systems of buried valleys formed by subglacial meltwater erosion have been documented at several locations on Mors by a combination of borehole logs and TEM data (Jørgensen & Sandersen 2004). The buried valleys on Mors are onshore equivalents of those described in the North Sea by Huuse & Lykke-Andersen (2000) and elsewhere in Jutland by Sandersen & Jørgensen (2003) and Jørgensen & Sandersen (2004). The valleys on Mors have a variety of orientations and dimensions. Most of them are incised into pre-Quaternary clay-dominated sediments and over the salt diapir the valleys are eroded into the chalk and limestone. The valleys are filled with glaciofluvial deposits, glaciolacustrine deposits, interglacial deposits and tills. Extensive glacial erosion is also evident above the central part of the salt diapir where tertiary sediments are absent (Elkraft & Elsam 1981; Gravesen 1990, 1993).

Quaternary deposits

The thickness of the Quaternary succession varies significantly as a result of glacial erosion and deformation. The deposits in the buried valleys are commonly more than 150 m thick, but where no valley erosion has taken place they can be less than 20 m thick. The cover is very thin or absent above the salt diapir. The majority of the Quaternary deposits are tills, but large amounts of glaciolacustrine clay and glaciofluvial sand and gravel are also present (Gravesen 1990, 1993). Interglacial deposits of marine clays occur locally. Such deposits are found in boreholes on the central southern part of Mors and are estimated to be of Late Elsterian–Early Holsteinian age (Peter Konradi, personal communication 2004). Stratigraphic investigations carried out at several cliff sections around the coast of Mors have demonstrated the occurrence of tills from the Weichselian, Saalian and Elsterian glaciations (Gry 1979; Ditlefsen 1991; Klint & Pedersen 1995; Pedersen 1996; Houmark-Nielsen 1999, 2003; Korsager 2002). In the area of the southwestern Limfjord just south of Mors, Late El-sterian–Holsteinian glaciolacustrine and marine clays are found at several locations (e.g. Jensen 1985; Ditlefsen 1991; Larsen & Kronborg 1994). It has been proposed that these sediments are deposited in a large system of glacial lakes and interglacial fjords (Larsen & Kronborg 1994).

Apart from a commonly occurring truncating upper till, most of the Quaternary sediments are disturbed and displaced by glaciotectonism. The discordant till indicates that the deformation was followed by transgression of the Late Weichselian Main Advance (e.g. Gry 1979; Ditlefsen 1991; Pedersen 1996; Korsager 2002).

The TEM method
Background

The Transient Electromagnetic (TEM) method was originally developed to explore mineral deposits in Canada and Australia in the 1960s and 1970s (Spies & Frischknecht 1991; Fountain 1998). The method is very suitable for mineral exploration, because of the high electrical resistivity contrast between host rocks and the mineralization. In hydrogeological mapping significantly lower resistivity contrasts must be resolved to identify differences in the clay content of the sediments, which are crucial when geological and hydrogeological models are to be constructed. Application of the TEM method to hydrogeological issues therefore requires high technical standards.

Some of the first groundwater surveys carried out by the use TEM were reported in the 1980s by e.g. Fitterman & Stewart (1986), Mills *et al*. (1988) and McNeill (1990). In Denmark the method was applied to hydrogeology in the early 1990s, as reported by Christensen & Sørensen (1998), Poulsen & Christensen (1999) and Sørensen *et al*. (2001a). During the 1990s, TEM became the preferred surveying method to obtain an overview of the general hydrogeological environment in an area to be investigated. Compared to other mapping methods, TEM is relatively cheap, it has a large depth of penetration and it provides both structural and lithological information. It cannot, however, provide the same amount of structural detail as the more costly seismic methods (Jørgensen *et al.* 2003a).

The Danish counties are responsible for water supply administration in Denmark, and an intense mapping campaign has been carried out since 2000. About one third of Denmark will be mapped before 2010–12. The TEM method is one of the key geophysical methods in this hydrogeological mapping campaign,
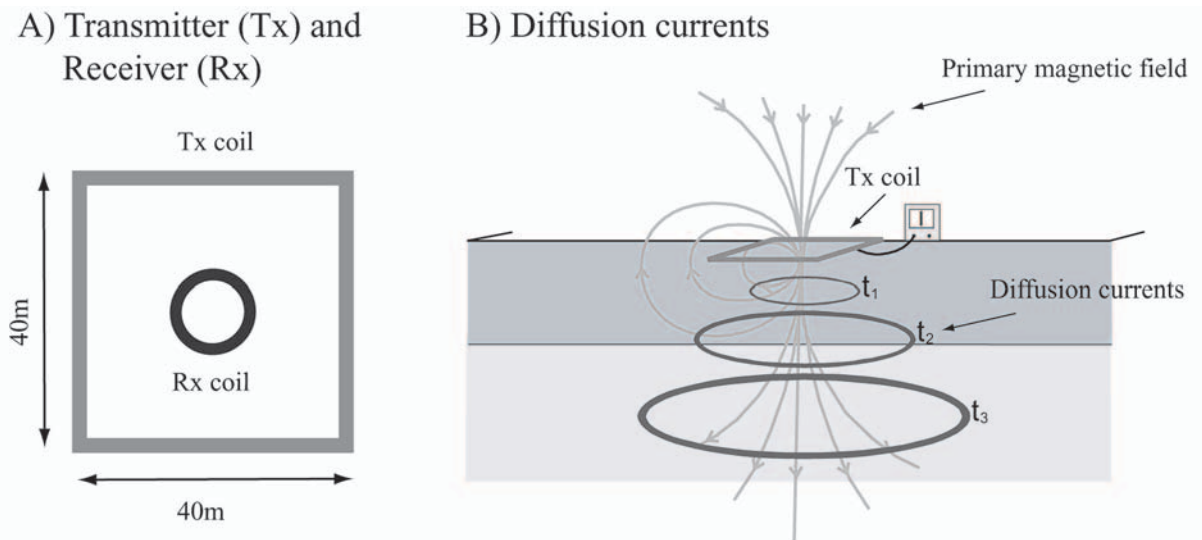
Fig. 3. A. Sketch of the TEM equipment setup. The transmitter (Tx) coil is typical 40 x 40 m². The receiver (Rx) coil is located in the centre of the Tx. B. Physics of the TEM method in a schematic view. The induced currents in the ground are illustrated as loops at three successively increasing times.

and most of the areas to be investigated will therefore be covered by TEM soundings. About 60,000 TEM soundings have been recorded so far, covering approximately 10% of the country.

Principles of TEM

A sketch of the TEM equipment setup is shown in Figure 3A. The receiver loop is located in the centre of the transmitter loop. The physics are illustrated in Figure 3B. A steady (primary) current is set up in the transmitter loop. At time zero this current is abruptly turned off, and (secondary) currents are induced in the subsurface. As time passes, the secondary currents diffuse downwards and outwards in the subsurface, and their magnitude is decreased because of conversion to heat. According to Faradays Law, the decaying secondary currents produce a (secondary) magnetic field which is measured as a voltage in the induction receiver coil. The voltage is measured as a function of time from the turn-off of the primary current.

A typical measurement is made from 10 ms to about 5 ms. The earliest measuring time depends on how fast the transmitter is able to turn off the primary current, and the latest time depends on the magnitude of the measured voltages versus the background noise level at the sounding site. The penetration depth is typically 120–150 m for a 40×40 m² transmitter loop utilizing 3 A. The penetration depth is highly dependent on the resistivity of the subsurface and the background noise level (Spies 1989).

The TEM data is in general subject to one-dimensional inversion, where the subsurface is divided into layers of homogenous and isotropic electrical resistivity. Typically, the models consist of 3–5 layers. Detailed descriptions of the inversion procedures are given in Effersø *et al.* (1999), Danielsen *et al.* (2003) and Auken et al. (2004).

Enhancements in TEM instrumentation and geophysical interpretation

The TEM instrumentation used in Danish hydrogeophysical surveys has undergone an intense development during the last few years (see Danielsen *et al.* (2003) for a detailed review). The 'conventional 40×40 TEM' configuration has been used since the very first Danish surveys. The system uses the Geonics PROTEM 47 receiver with a single-turn 40×40 m² transmitter loop with the receiver coil placed in its centre. The penetration depth attained by this setup is 120–150 m, and the standard spatial coverage is 16 soundings per km². The design of the system and the data coverage form a compromise between providing sufficient resolution of the subsurface, data quality and an acceptable cost of the survey.

The conventional 40×40 TEM configuration is still used in some surveys, but new TEM systems have gradually taken over to provide for deeper penetration and higher spatial coverage at the same or lower costs. The most prominent of these systems is the HiTEM system (Danielsen *et al.* 2003) which has penetration depths down to 250–300 m. While the HiTEM

system is a single-site system, the PATEM and the successor SkyTEM system (Sørensen & Auken 2004; Sørensen *et al.* in press) measures continuously along profiles. In its current development stage the SkyTEM system has a similar penetration depth to the HiTEM system, but data are measured continuously while the system is moved by helicopter. Obtaining measured data continuously greatly increases the data quality and resolution of the subsurface.

This development in instrumentation has been accompanied by a similar intensive development of interpretation algorithms. Where the single-site measurements were inverted and processed independently (HydroGeophysics Group 2004a), the continuously measured data can be inverted along profiles using the Laterally Constrained Inversion (LCI) approach (Auken & Christiansen 2004; Auken *et al.* 2004). In the LCI approach, layer resistivities and layer boundaries are tied together with a space-dependent variance reflecting the natural variations of the resistivity properties of the subsurface. The outcome is geophysical models where the problems with layer suppression and resistivity equivalences are significantly reduced.

Resolution of layers and structures

Because the TEM method mainly resolves and quantifies low-resistive layers, values for layers with resistivities exceeding 80–120 ohm-m are not precisely determined; they just have 'high' resistivity. Furthermore, for certain combinations of layer thicknesses and resistivities, equivalence problems make it impossible to determine either the exact thickness or resistivity of the layers (Fitterman *et al.* 1988).

Like all electromagnetic diffusion methods TEM has a decreasing resolution capability with depth. As a rule of thumb, layers with a thickness of 15–20 m can be resolved in the shallow part, while layers must be more than 20–50 m thick to be resolved at 100 m depth. Individual geological layers will commonly be averaged into one model layer because geological layers are normally too thin to be resolved. In general, 3–5 layers can be satisfactorily resolved in a TEM sounding. Furthermore, under normal circumstances the upper 10–20 m will be averaged into one layer, due to principal difficulties in recording data at very early decay times. The above-mentioned numbers are very dependent on the resistivity of the layers. The lateral resolution capability of 3-D structures also decreases with depth. At depths of about 100 m the area from which data is obtained is more than 300–400 m in diameter. For depths of 25 m the area only 75–100 m in diameter. This implies that 3-D

structures are less resolvable and become more diffuse with depth. Modelling of 2- and 3-D structures has been thoroughly discussed by e.g. Newman *et al.* (1986), Goldman *et al.* (1994), Danielsen *et al.* (2003) and Auken *et al.* (2004).

Presentation

In order to facilitate geological interpretations the inverted models are typically presented in thematic maps and cross-sections. The resistivities as estimated by the inverted models do not provide unambiguous information about lithology in the subsurface layers, and they have to be interpreted by the use of different types of thematic maps. Those most commonly used are interval resistivity maps and maps of depths to low-resistive layers. Interval resistivity maps are normally produced in 10 or 20 m elevation intervals, where average resistivities are calculated within each interval. Such short intervals are required for an optimized interpretation because some layer boundaries, especially those defining the surface of the low-resistive layer, are normally very well determined (within 10 m, see below). A complete succession of intervals covering the subsurface down to the maximum depth of penetration has proved to be a useful way to visualize the TEM survey results as a basis for geological interpretations (GeoFysikSamarbejdet 2003, Jørgensen *et al.* 2003b). The interval resistivity maps are typically supplemented with depth control maps of a low-resistive deep-seated layer, if such a layer exists. This depth control map shows the elevation of a selected layer, where the selection is the deepest layer in all inverted models with resistivities below a given level.

A cross-section presentation is often used when TEM data are compared with other types of data or if detailed studies of the resistivity models are needed in selected areas. Just like borehole logs, TEM-models are most commonly shown on the sections by narrow vertical panels (e.g. GeoFysikSamarbejdet 2003; Jørgensen et al. 2003a; Sandersen & Jørgensen 2003). Another useful way to display the TEM survey results on cross-sections is to transfer a dissected succession of interval resistivity maps onto the sections.

Geological interpretation of TEM surveys

Experience from geological interpretation of TEM surveys is primarily gained when their results are compared with other types of data sets, especially from boreholes. Large numbers of TEM surveys car-

ried out in Denmark have contributed significantly to the understanding of how the resistivity images of the subsurface can be interpreted in geological terms (Auken *et al*. 2003; GeoFysikSamarbejdet 2003; Jørgensen *et al*. 2003a, 2003b; Sandersen & Jørgensen 2003; Jørgensen & Sandersen 2004).

The electrical resistivity of sediments is controlled by clay minerals in the matrix and the ion content of pore water. If the ion content of pore water can be taken to be low and relatively constant in a survey area, information about the clay content may be achieved. This information, however, depends on both the amount and nature of the clay. The role of the ion content of pore water on the formation resistivity is much more significant for coarse-grained sediments than for fine-grained sediments.

The hurdle for the geological interpretation of TEM-data is conversion from the modelled layer resistivities to the lithology of the layers and from layer geometry (as revealed by correlations between soundings) to structural reality. This conversion requires several aspects to be considered: 1) identification and exclusion of coupled and otherwise noise-infected soundings, 2) the vertical and horizontal resolution capability, 3) resistivity values of lithologies in the survey area, 4) ion content of the pore water. The principal means for achieving the geological interpretation are: 1) correlation with independent information from other data sets, 2) evaluation of the various thematic maps (as mentioned in the previous paragraph) in terms of independently derived and well documented geological models.

The lithological interpretation of the TEM survey on Mors is based on empirical comparisons between TEM data and borehole logs. A list of typical resistivities for some of the most common sediments occurring on Mors and in the adjacent areas is shown in Table 1. The resistivities are estimated for freshwater saturated sediments.

Data collection and data processing
Field surveys and data base

A total of 2904 TEM soundings were collected on Mors during the period 1998–2002. The field survey, data processing and modelling were carried out by the consulting company Dansk Geofysik for Viborg County (Dansk Geofysik 2002). The survey is part of an ongoing hydrogeological survey campaign designed to investigate aspects of groundwater resources. The average density of TEM soundings is around 11 per km^2. In four high-priority areas the density is 12–16 per km^2. These areas are situated in the far northern part, in the northern middle part, in the southern middle part and in the far southern part of the island (Fig. 4). Between the densely covered areas the density is about 5–8 soundings per km^2. Approximately 50% of the island is densely covered with soundings, 40% is sparsely covered, and the remaining 10% has not been investigated. The TEM instrumentation used for the survey is the Geonics PROTEM 47 system and the conventional 40×40 TEM

Table 1. Estimated resistivity values for freshwater saturated sediments in the Mors region. Modified from GeoFysikSamarbejdet (2003) and Jørgensen *et al.* (2003b).

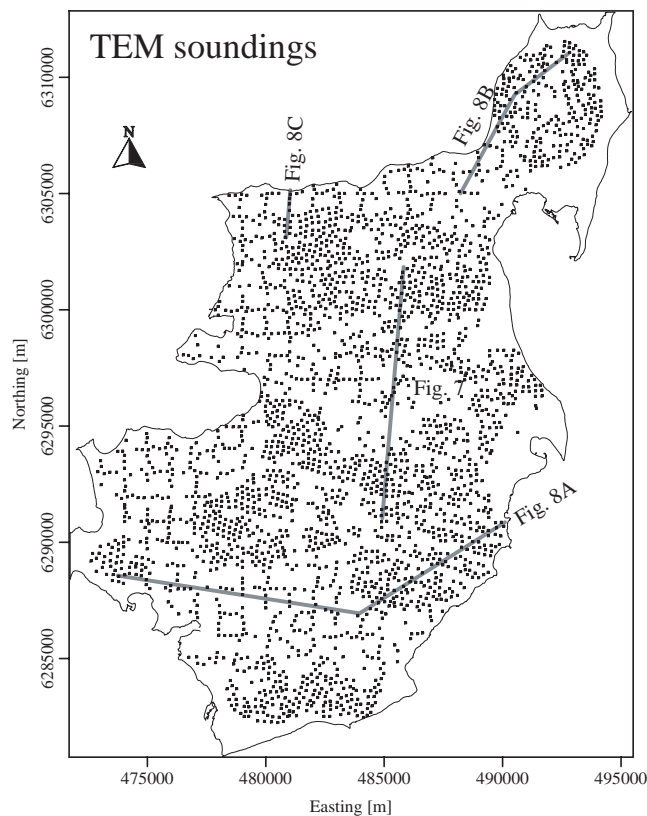| Sediments	Resistivity
Meltwater sand and gravel	> 60 ohm-m
Clay till	25–60 ohm-m
Glaciolacustrine and marine clay	10–40 ohm-m
Paleogene clay	1–10 ohm-m
Paleogene diatomite	10–40 ohm-m
Maastrichtian white chalk	30–100 ohm-m
Danian limestone	> 80 ohm-m

Fig. 4. Map showing all TEM soundings on Mors. Grey lines mark the cross-sections of Figure 7 and 8. Scale: 5 km between axis ticks. Coordinate system: UTM zone 32/ED50.

configuration was applied (Dansk Geofysik 2002). All collected TEM data have been reported to the national database of geophysical data GERDA (http://gerda.geus.dk), and the TEM data used here is an extract from GERDA provided by Viborg County.

Data processing

The extracted TEM data from GERDA has been carefully examined in order to remove noise-infected TEM soundings. A total of 249 TEM soundings have been classified as noise-infected and useless, primarily due to local transmitter coupling to man-made conductors or high levels of background noise (Sørensen *et al.* 2001b). Mainly capacitive coupled soundings with oscillatory data have been removed (see examples in Danielsen *et al.* 2003, figs 4, 5). Galvanic coupled data, however, can be impossible to identify, and a limited number of coupled soundings might therefore still be present in the dataset. After removal of the identified coupled soundings the remaining 2655 soundings constituted the basis for further interpretation.

All soundings have been inverted by the surveyors using 1-D inversion modelling code EM1DINV (HydroGeophysics Group 2004b; 2004c). The selected models contain the fewest possible layers within accepted limits of fit between model data and observed data. All models contain 2–5 layers. No a priori information from borehole logs or other geological information was used during the inversion process or in the selection of models. The models therefore represent objective datasets, without biased interpretation at this stage of the data handling process.

In the following the model estimation uncertainty is given as standard deviations on model parameters using the standard deviation factor, STDF (Auken & Christiansen 2004). A factor of STDF = 1 is the impossible case of perfect resolution. A STDF of 1.1 is approximately equivalent to an error of 10% and a STDF of 2 is approximately equivalent to an error of 100%. The median of the STDF for the depth resolution of all layers in all sounding models is 1.11. For resistivities the same value is 1.17. About 17% of all depth estimations have STDF > 2 and about 21% of all resistivity estimations have STDF > 2. Layers with low resistivities are better resolved than high-resistive layers. The depth to the bottom layer, which in most soundings is low-resistive, is therefore well resolved. The median of the depth to this layer is 1.05 STDF and only 1% of the values are poorly defined with a STDF > 2.

With the geophysical data and models in GERDA and by use of the newly developed modelling and presentation program, Workbench, (HydroGeophysics Group 2004d), it is possible to construct a variety of thematic geophysical maps and profiles targeted at specific geological environments.

The geological modelling presented here is mainly carried out on the basis of interval resistivity maps representing intervals of 10 m. Elevation maps of low-resistive layers are used. The maps of low-resistive layers are generated on the following basis: 1) The layer resistivity of the selected layer must be less than 10 ohm-m, 2) the layer below must not exceed 10 ohm-m, and 3) the layer search routine is conducted from the top downwards. The 10 ohm-m-limit is chosen because the Paleogene clay layers in the area normally exhibit resistivities below 10 ohm-m.

Kriging interpolation with cell spacing of 125 m and a search radius of 600 m is used for the gridding of the thematic maps. Colour scales with reddish colours for high-resistive layers and bluish colours for low-resistive layers are used, whereas for the elevation maps reddish colours show high levels and bluish colours show low levels.

To support the geological interpretation of the TEM data all relevant and available data and information are taken into account. Examples are borehole logs from the national well database "Jupiter" (GEUS 2003), results from field investigations in clay pits and coastal cliffs, as well as other geological investigations and relevant literature. The locations of all referenced boreholes in the text are shown in Figure 5B.

Results and discussions

Results of the survey are outlined in an elevation map of the deepest low-resistive layer (Fig. 5A) and four selected maps of interval resistivity (Fig. 6A). It is not possible to show all interval resistivity maps of the succession, and the selected maps are therefore chosen to emphasize the most vital information. Sketches illustrate layer boundaries and geological structures seen in the maps (Figs 5B, 6B). They do not show the overall interpretations, but outline only what can be observed directly on the individual maps. They are meant as a guide for the descriptions, as are the letters and numbers annotating the various features.

The elevation map (Fig. 5) shows the deepest low-resistive layer (resistivity lower than 10 ohm-m). From borehole logs it appears that, in most of the island, this layer can be correlated with Paleogene clay, but occurrences of saline groundwater in sand/
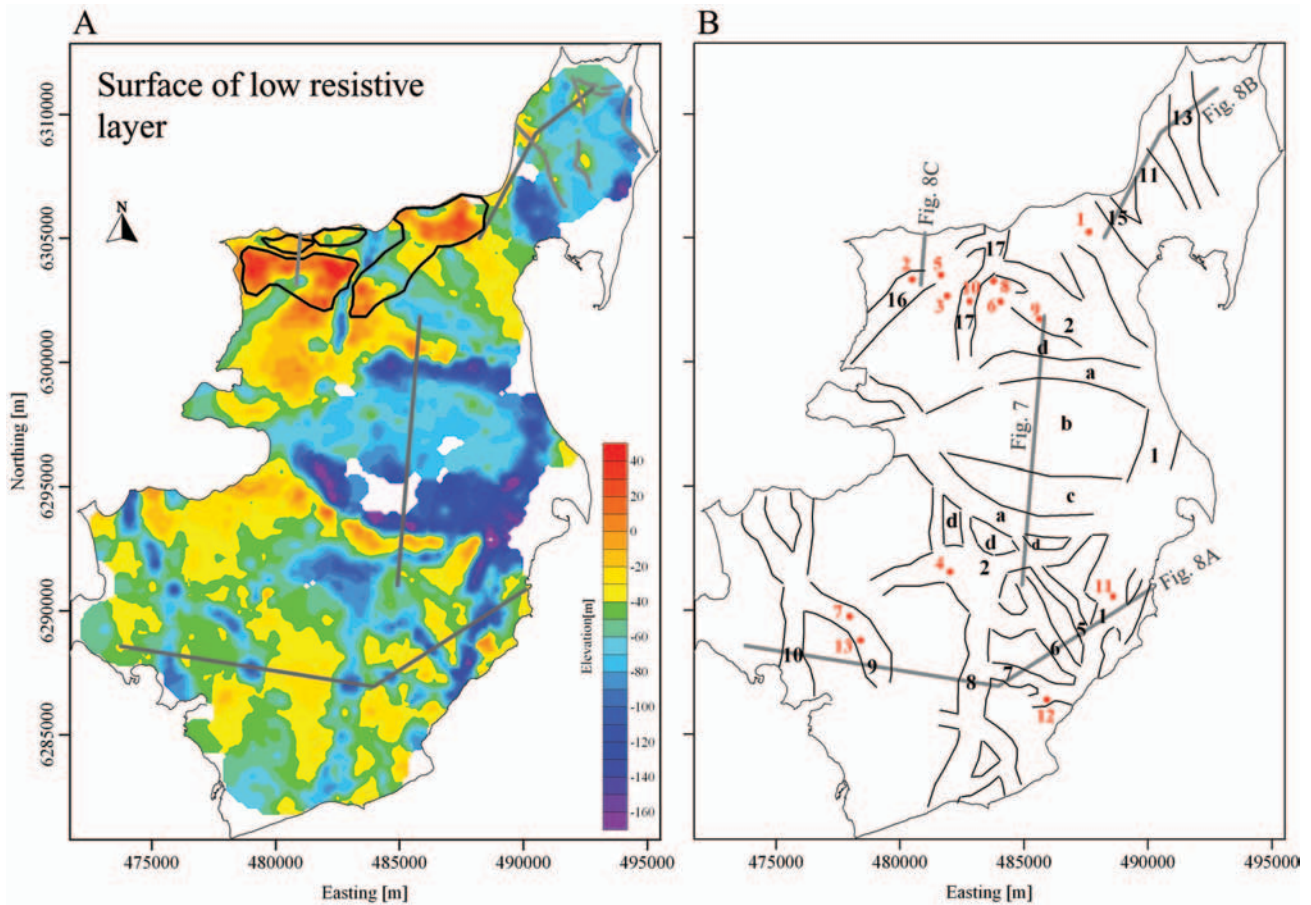
Fig. 5. A. Thematic geophysical map showing the level of the deepest layer in the TEM models with resistivities lower than 10 ohm-m. Cross-sections in Figure 7 and 8 are shown as thick grey lines. Areas of composite-ridge systems in the Hanklit area are marked with black polygons. Grey lines mark ice-marginal moraines in the northeastern part of the island. B. Outlines of structures and geological elements referred to in the text are shown on the sketch with black lines, numbers and letters. Boreholes mentioned in the text are marked with red dots. The borehole numbers refer to the Jupiter well database (GEUS 2003) as follows: 1: 30.949; 2: 37.617; 3: 37.760; 4: 37.771; 5: 37. 816; 6: 37.850; 7: 37.853; 8: 37.1049; 9: 37.1241; 10: 37.1242; 11: 37.1248; 12: 45.418; 13: 45.533. Scale: 5 km between axis ticks. Coordinate system: UTM zone 32/ED50.

gravel or chalk/limestone may locally influence the image of the low-resistive layer. The map therefore shows the topography of the Paleogene clay surface with local influence by saline groundwater. Such occurrences are mainly seen in the layers over the salt diapir. The elevation of the low-resistive layer ranges from more than 170 m b.s.l. to approximately 50 m a.s.l.

The four interval resistivity maps (Fig. 6A) show a vertical distribution from low resistivities in the deeper layers to generally high resistivities in the shallow layers. This illustrates the general succession of tertiary and Quaternary sediments in the area, gradually changing from clay dominated layers at depth to more sandy layers in the upper parts. The appearance of the large-scale geological features in the TEM survey (the Mors salt diapir, the buried valley systems, and the glaciotectonic complexes) is

described and analyzed below. The appearance of the individual features in the TEM images is presented, and the descriptions are then compared to lithological information derived from borehole logs, exposures, etc.

The Mors salt diapir

The salt diapir in the TEM survey. Two curved depressions appear on the elevation map of the deepest low-resistive layer in the central part of Mors (Fig. 5, structure a). Together, these two curved depressions form an elliptic shape open to the east and the west. The curved depressions are more than 150 m deep and between 5 and 10 km in length. To the east they merge into a long linear depression (structure 1), and to-

Jørgensen *et al.:* Geological mapping of Mors, Denmark – Study on a large-scale TEM survey   · 61
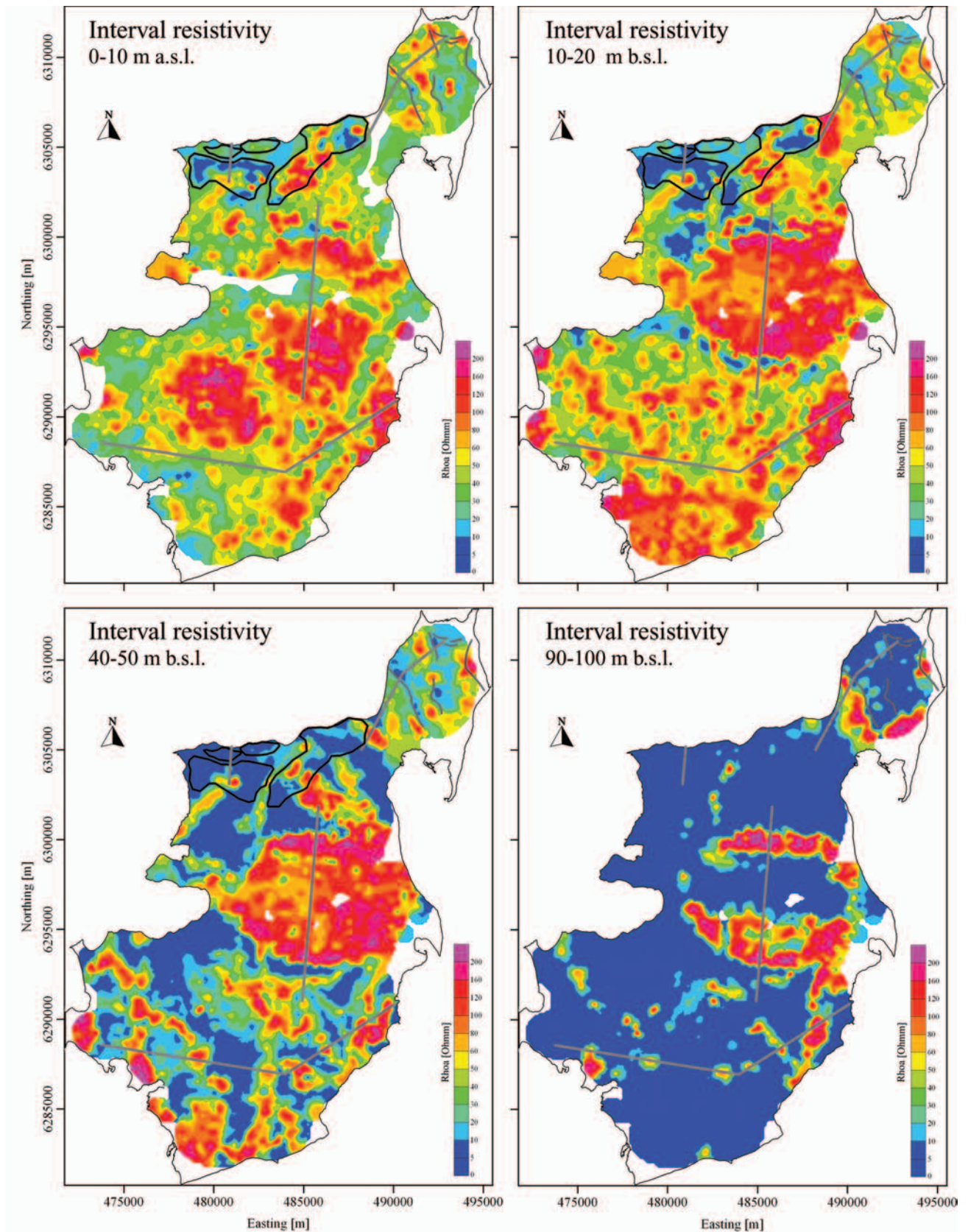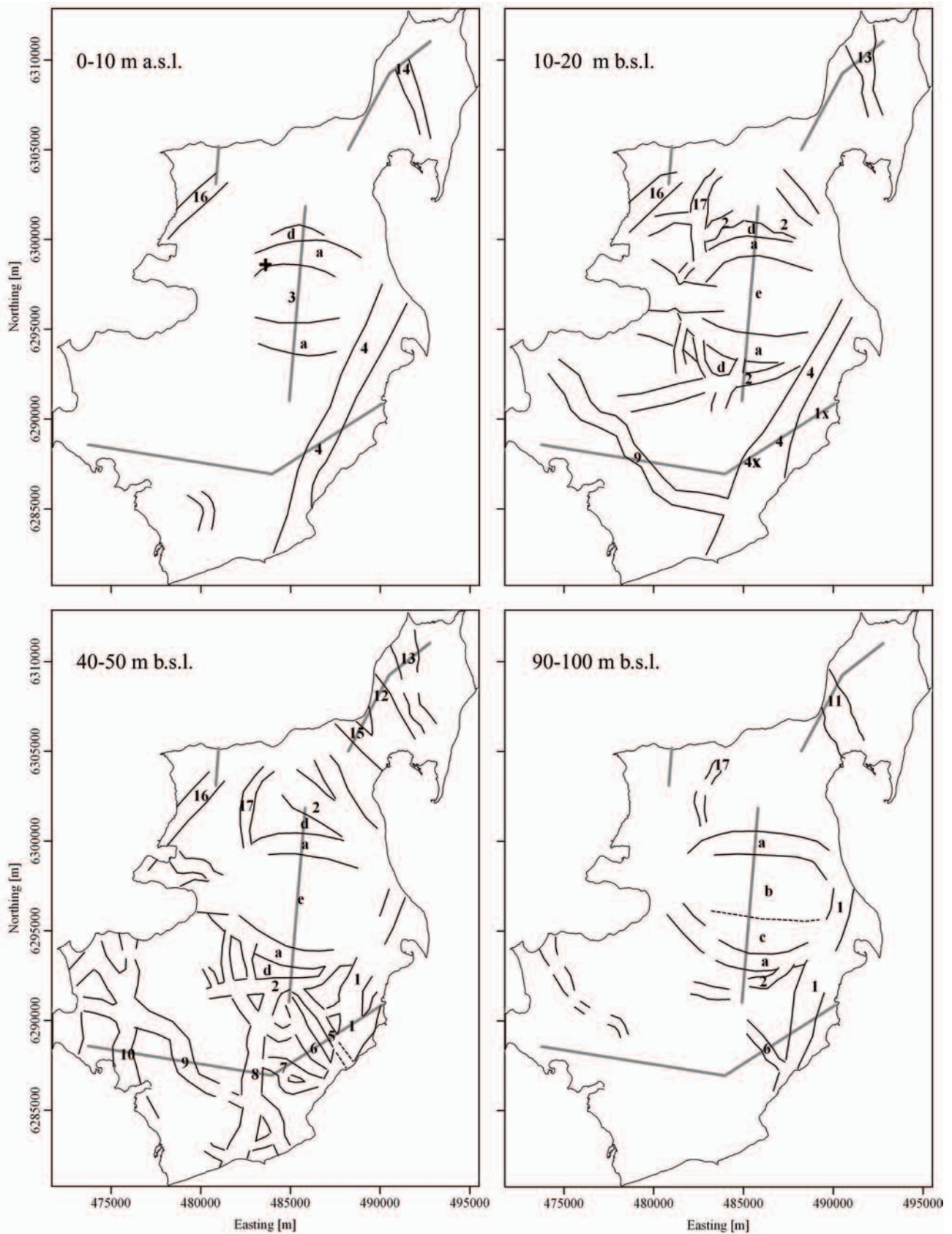
Fig. 6. A. Geophysical thematic maps showing the average resistivities in selected intervals. The TEM soundings do not penetrate more than about 30–50 m into the Paleogene clay layers (blue), and the data coverage is therefore sparse in the low resistive areas of the deepest interval of 90–100 m b.s.l. Cross-sections of Fig. 7 and 8 are shown as thick grey lines. Areas of composite-ridge systems in the Hanklit area are marked with black polygons. Grey lines mark ice-marginal moraines in the northeastern part of the

island. Coordinate system: UTM zone 32/ED50. B. Outlines of structures and geological elements referred to in the text are shown on the sketches with black lines, numbers and letters. The + on the interval of 0–10 m a.s.l. shows the location of a chalk pit at Erslev. Scale: 5 km between axis ticks.
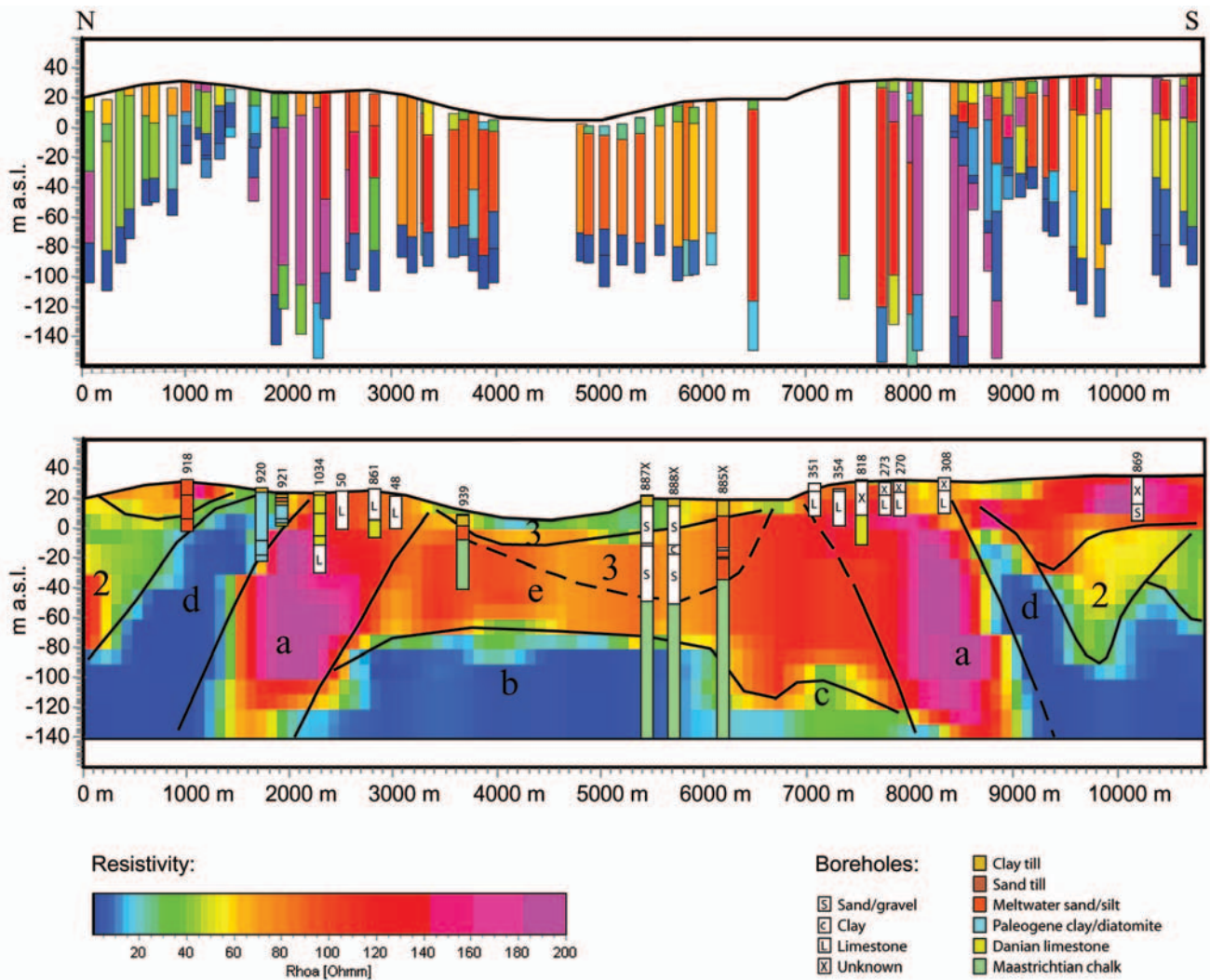
Fig. 7. Cross-section across the Mors salt diapir. The upper panel shows the single resistivity models of each TEM sounding situated within less than 300 m from the section line shown which is in Figure 4, 5 and 6. The lower panel shows the succession of interval resistivity grids as they are cut vertically by the cross-section. The TEM soundings do not penetrate more that about 30–50 m into the Paleogene clay layers (blue). The panels, however, show the interpolated resistivity grids down to -140 m a.s.l. regardless of the limited penetration into the Paleogene clay. Interpretations and geological elements referred to in the text are marked on the lower panel with black lines, numbers and letters. Lithological data from selected borehole logs are projected and superimposed onto the section from distances of up to about 500 m. The annotated borehole numbers with prefix '37' refer to the national archive of borehole logs, Jupiter (GEUS 2003). Note the considerable vertical exaggeration: 15 x.

wards the west they terminate abruptly. Between the two depressions the surface is slightly higher (Fig. 5, structure b), except for an area close to the southernmost depression (Fig. 5, structure c). The surface of structure b is located at around 50–80 m b.s.l. The southernmost depression is flanked by a prominent ridge, and the same applies to the western part of the northernmost depression (Fig. 5, structure d). The ridges are intersected by other elongate depressions with straight or irregular forms, and two relatively large elongate depressions are located more or less parallel to the ridges (Fig. 5, structure 2).

Figure 7 shows a cross-section through the area described above. The upper panel in the figure shows the individual TEM models, and the lower panel shows the entire stack of interpolated interval resistivity grids of which four intervals are shown in Figure 6. Geological interpretations are outlined by line drawing superimposed on the lower panel. The dark blue colours in the section represent the low-resistive layer whose surface was shown in Figure 5. The two curved depressions (structure a) appear in Figure 7 as dipping layers with very high resistivities (>120 ohm-m), between which two more or less flat-

topped bodies of low resistivity can be seen (structure b and c). The ridges of structure d occur as dipping layers resting on structure a, and the elongate depressions outside the ridges (structure 2) are, at least in the southern part, seen as a V-shaped structure with varying resistivity. The impression given by the cross-section is that the high-resistive structures of dipping layers converge towards a common point at around 100 m a.s.l.

Most of the structures described are also seen in the interval resistivity maps (Fig. 6). In the highest level (0–10 m a.s.l.) the structures of a and d are seen as curved bodies with high and low resistivities, respectively. Structure d, however, only occurs towards the north, and structure a is diffuse, especially to the south. Between these, there is a structure with slightly lower resistivities (20–40 ohm-m; structure 3) which is also seen in the cross-section (Fig. 7). Another elongated structure of relatively low resistivity (structure 4) cuts the southeastern part of structure a.

The structures of a and d become more distinct in the interval of 10–20 m b.s.l. Structure d is dissected by several elongate elements with high resistivities which were seen as depressions in the low-resistive layer (Fig. 5). Structure 2 also appears at this level, but structure 4 is less significant. Structure 3 is not seen but layers with medium-to-high resistivities (60–140 ohm-m) are observed instead (structure e).

Between 40 and 50 m b.s.l. the low-resistive layer begins to dominate the succession. Structure a is even more distinct, and structure d gradually merges into the low-resistive layer in general. Structure 2 becomes more well-defined, and structure 1 gradually appears. Apart from structures a, c, 1 and 2, the low-resistive layer dominates the image in the lowermost slice at 90–100 m b.s.l. Due to the dipping layers the distance between the arcs of structure a gradually increases downwards through the intervals. In the uppermost slice, the maximum distance is around 3.5 km while at the deepest level it expands to about 5.5 km. The exact inclination of the layers is, however, difficult to assess, because of the difficulties of the TEM soundings to penetrate the low-resistive layers properly at great depths. Given this reservation the mean inclination of the layers is estimated to be about 5°.

Interpretation and lithology. The Mors salt diapir was previously described on the basis of mainly low resolution seismic surveys (e.g. Elkraft & Elsam 1981; Larsen & Baumann 1982), deep exploratory drillings (Elkraft & Elsam 1981) and the national archive of borehole logs (Gravesen 1990, 1993). The diapir is situated in the central part of Mors, exactly where the dipping layers appear in the TEM data. Several boreholes penetrate the upper parts of the succession in the area, and from this it can be concluded that structure a corresponds to Danian limestone, and structures b, c and e correspond to Maastrichtian white chalk (compare with superimposed boreholes on the lower panel, Figure 7). The boundary between the Danian and the Maastrichtian is exposed at about 10 m a.s.l. in a chalk pit at Erslev (Andersen & Sjørring 1992), and this level is consistent with the uppermost interval in Figure 6. The location of the pit is marked with a cross on this interval map, and it is seen to correlate exactly with the inner/lower limit of structure a. Structure d corresponds to Paleogene clay layers, locally glaciotectonically deformed into large fold structures (Pedersen 2000). No boreholes, however, penetrate structure d on the southern flank, but this can by analogy also be interpreted as Paleogene clay.

The structures of 1 and 2 correspond to various glacigenic sediments, but structure 4 appears more homogeneous and consists of meltwater clay, although described as tertiary clay in some borehole logs (see discussion below). Apart from relatively thin, scattered occurrences of Postglacial sediments, structure 3 also corresponds to glacigenic sediments, but this structure is mainly composed of clay till. The glacigenic sediments extend downwards into structure e, but this cannot be seen in the TEM images at deeper levels because here the sediments gradually become more sandy, resulting in an insignificant electrical contrast to the underlying chalk of medium to high resistivities. In Figure 7 the boundary between glacial sediments and chalk is estimated from borehole data and marked by a dashed line. The structures 1, 2, 3 and 4 can be characterized as buried valleys, as described by Jørgensen & Sandersen (2004). Locally, where the valleys incise the covering layers, the diapir becomes diffuse and difficult to see in the TEM soundings. Buried valleys will be more thoroughly described below.

The low resistivities of structures b and c indicate that the chalk contains highly saline pore water which has not been leached by circulating groundwater. The salt-freshwater boundary is located between 50 and 80 m b.s.l. over the northern part of the salt diapir (structure b), but to the south it seems to be located as deep as 120 m b.s.l. (structure c). The deepening of the salt-freshwater boundary to the south can probably be explained by differences in the level of the groundwater table which to the south, above structure c, rises gradually from about sea level to 5–10 m a.s.l. Other explanations could be the presence of faults and/or differences in lithology and permeability, whereby the salt water locally could have been removed. Geoelectrical soundings and resistivity logs

in deep boreholes previously estimated the salt-fresh-water boundary to be located about 50 m b.s.l. below Lyngbro Bæk over the central part of the diapir and deeper to the south and north (Elsam & Elkraft 1981). This is consistent with the results presented here.

The Danian limestone (structure a) is in general expected to be more coarse-grained and fractured than the white chalk. The hydraulic conductivity is therefore significantly higher in the limestone and the leaching of saline pore water may be effective to greater depths here. The deepest level of fresh ground-water in the limestone cannot be detected by the TEM soundings because only high resistivities occur within the assumed penetration depth of 120–140 m b.s.l. From the section (Fig. 7) it can be directly deduced that the stratigraphic thickness of the Danian limestone is about 80 m.

Erosion. The cover layers of the Mors salt diapir are clearly imaged in the TEM survey. The flanking Danian limestones and Paleogene deposits appear with high and low resistivities, respectively. Due to erosion these layers are not present over the central part of the diapir where Maastrichtian chalk is exposed directly below glacial sediments. As observed in the section (Fig. 7) the missing layers over the salt dome comprise at least the Paleogene clay, Danian limestone and an upper portion of the chalk. The missing section can be calculated to represent a thickness more than 200 m over the central part of the diapir. Extensive erosion must be responsible for the removal of this material. The erosion must have taken place some time during Neogene or early to middle Pleistocene and could possibly be the local effect of the regional late Cenozoic erosion, which is estimated to have had a magnitude of 500–750 m in the Mors area (Japsen & Bidstrup 1999). An east-west striking valley structure filled with glacial deposits is situated in the chalk centrally over the diapir. This valley may reflect a graben structure formed by dissolution of salt and/or by extension during the uplift. If so, the amount of erosion could be slightly lower than estimated because some of the missing layers would have been subjected to subsidence instead of erosion. Another open question is whether the erosion may have been restricted to the area over the salt diapir during uplift, and not related to the regional late Cenozoic erosion.

Buried valleys

Buried valleys in the TEM survey. Buried valleys incised into the layers above the salt diapir have been described above. Here we consider buried valleys on the entire island. In the interval resistivity maps (Fig. 6A), valley structures appear as elongated bodies defined by resistivity contrasts to their surroundings (compare with Figure 6B). These bodies mainly show moderate to high resistivities, but fairly low resistivities also occur, especially at the higher levels. The deepest incised valley structures are clearly expressed in the surface of the low-resistive layer as blue/green elongate features (Fig. 5).

Beside the thematic maps, two cross-sections presented in Figure 8 demonstrate the occurrence and nature of these valleys. One cross-section is located in the southern part of the island (Fig. 8A), and the other in the northeastern part (Figs 4–6, 8B). The cross-section located in the southern part of the island (Fig. 8A) crosses a number of buried valleys. At the eastern end it crosses the deep valley structure described as structure 1 above. The valley contains deposits of high resistivity, and in the cross-section, as well as in the horizontal images, it is clear that it constitutes more than one incision. Structure 1x is a younger valley structure, which seems to be quite shallow. Structure 4, which was seen as an elongate structure of low-to-medium resistivities in the upper part of the succession (Fig. 6), occurs in the section at 13500 m. The downward narrowing of this structure through the TEM intervals is characteristic for buried valleys. There is another elongate structure parallel to the southern part of structure 4. This feature, named structure 4×, contains deposits of high resistivities and is partly seen in the interval of 10–20 m b.s.l. (Fig. 6).

In the surface of the deep low-resistive layer, a group of other buried valleys appear below the valley of structure 4 (Fig. 8A). Of these valleys, structure 5 is shallow whereas structures 6 and 7 are deep, reaching depths of about 120. m. b.s.l. The three valleys are clearly seen (Figs 5, 6 (40–50 m b.s.l.)) where they appear to diverge towards west and northwest. Three more valleys (structure 8–10) occur in the western part of the cross-section (Fig. 8A). These, as well as the other deep valleys, are filled with deposits of high resistivity. Their deeper parts are incised into the low-resistive layer, whereas their upper parts appear to incise layers with medium resistivities. The valleys seem to terminate upwards at a level corresponding to the present-day sea level, and they reach depths of about 120 m b.s.l. They are clearly seen in the surface of the deep low-resistive layer (Fig. 5) and in the interval resistivity level of 40–50 m b.s.l. in Figure 6. Structure 9, striking SE-NW through the southern part of the island, does also occur in the interval resistivity level of 10–20 m b.s.l. Structures 8 and 10 are oriented N-S.
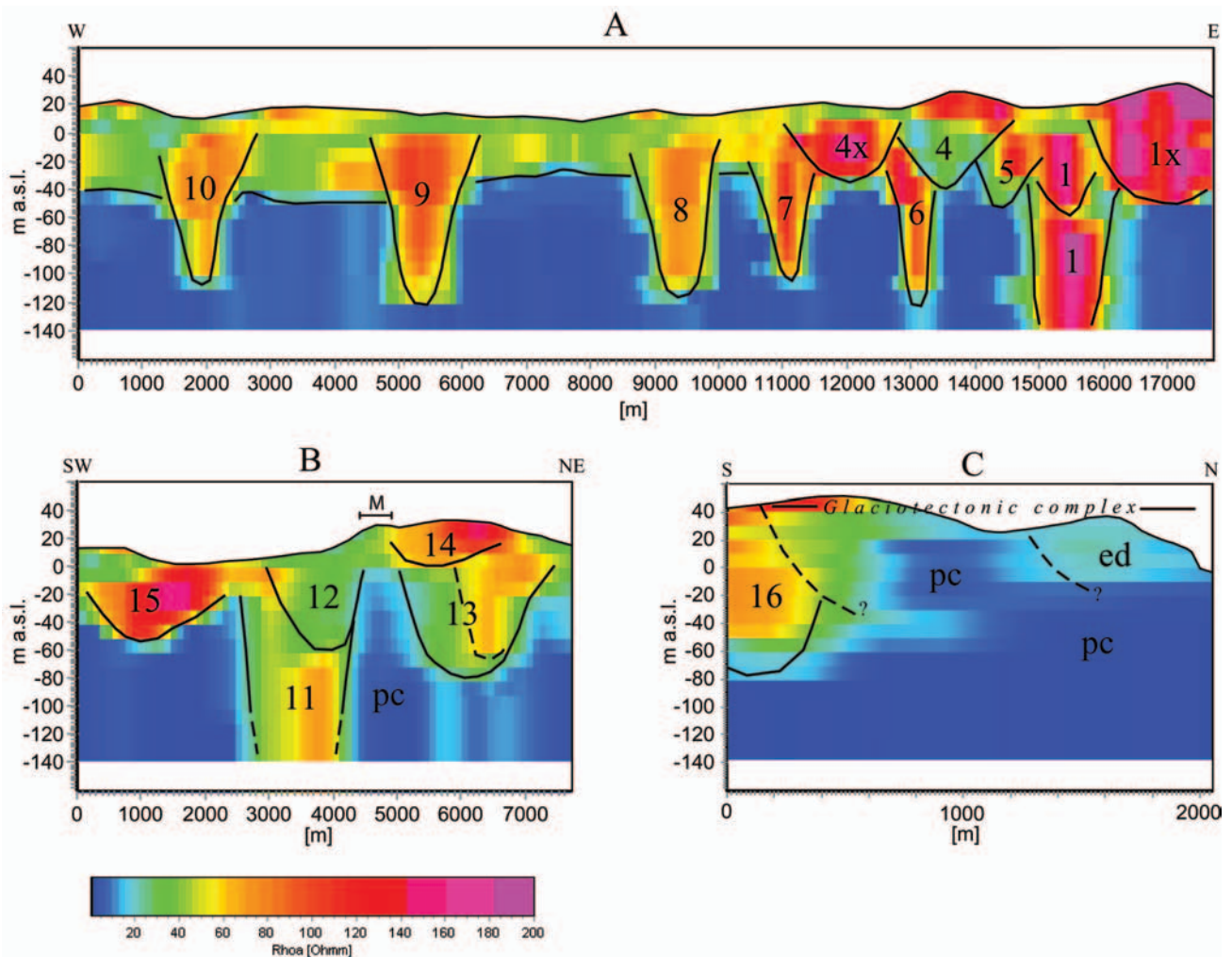
Fig. 8. Two cross-sections (A and B) showing buried valleys in the southern and the northern part of Mors respectively, and one cross-section (C) through a glaciotectonic complex in the Hanklit area. The panels show the successions of interval resistivity grids as they are cut vertically by the cross-sections. The TEM soundings do not penetrate more that about 30–50 m into the Paleogene clay (dark blue). The panels, however, show the interpolated resistivity grids down to -140 m a.s.l. regardless of the limited penetration into Paleogene clay. Interpretations and geological elements referred to in the text are marked by black lines, numbers and letters. 'M' denotes ice-marginal moraine at Skærbæk Klint. Note the considerable vertical exaggeration (22 x) for sections A and B. For section C the vertical exaggeration is approximately 5×.

Significant incisions into the low-resistive layer also occur on the northern cross-section (Fig. 8B). The largest valley structure in this cross-section is located between 2500 m and 4300 m where deposits of medium-to-high resistivities (structure 11) are seen at depths of up to 120–140 m b.s.l., and layers with medium resistivities (structure 12) are present above 60 m b.s.l. The exact depth of this valley is uncertain because no TEM soundings have been able to detect the valley bottom. Other valley features are seen in the northeastern part of the section, where one or two valleys (structure 13) cut down into the low-resistive layer, while others (structure 14) seem to incise only the top of the succession. Finally, a quite shallow valley filled with high-resistive deposits is

seen in the southwestern part of the section (structure 15). The valley features detected in the northern cross-section (Fig. 8B) can also be seen in the surface of the low-resistive layer (Fig. 5) and in the interval resistivity maps (Fig. 6). They appear as elongated depressions and bodies with varying resistivities. However, not all valleys in the section are equally distinct on the maps, and there may therefore be other explanations for some of these features (see discussion below). Only a fraction of the buried valleys located in the TEM survey have been described above. Most of the valleys are outlined in the thematic maps (Figs 5, 6) but not all identified valleys are shown due to limitations in the number of thematic maps presented here. Some valleys, for example, only ap-

pear in limited intervals at levels between the selected intervals. Furthermore, only valleys with a significant resistivity contrast between the infill and the surroundings can be detected by the TEM method (Jørgensen *et al.* 2003b). It is also necessary that the valley fill consists of relatively homogeneous sediments without sections with varying resistivities, leading to inconsistent resistivity contrasts.

The buried valleys found on Mors vary with respect to both dimension and orientation. Their depths vary from a few tens of metres to more than about 140 m. Their widths are normally between 500 and 1500 m, but some are up to 3000 m wide. The trends of the valleys are mostly restricted to the orientations N-S, SE-NW and E-W. In valley intersections it can occasionally be observed that younger valleys erode into the infill of older valleys.

Lithology of the valleys. As described above many structures appearing in the thematic maps can be identified as buried valleys, solely on the basis of their shapes. However, it is necessary to combine the TEM data with lithological information from boreholes in order to make a proper interpretation. Information from the national well database (Gravesen 1990, 1993; GEUS 2003) is therefore taken into account and compared with the TEM data. Most boreholes are poorly described lithologically and only few of them reach depths of more than 50 m. Nevertheless, many borehole logs provide useful information about the valley infill as well as the incised substratum.

Except for the central area over the salt diapir and a few areas close to the sea, the deep-seated low-resistive layer (Fig. 5) correlates with Paleogene clay in the borehole logs. However, in places where diatomite dominates the upper part of the Paleogene, discrepancy between the Paleogene surface and the low-resistive layer may occur. The reason is that diatomite normally exhibits resistivities higher than 10 ohm-m (see Table 1). In the coastal areas, saline pore water at deep levels may lead to erroneous geological interpretations. The low resistivities, e.g. below structure 1×, can therefore be a result of saline pore water, and the valley may be deeper than it appears on the TEM images.

According to the borehole logs the valley fill deposits are all of Quaternary age. High resistivities (> 60 ohm-m) appear in general to be dominated by meltwater sand and gravel; medium resistivities (40–60 ohm-m) are normally found to be deposits dominated by clay till or mixed deposits, whereas layers with low-to-medium resistivities (10–40 ohm-m) are dominated by lacustrine clays of glacial, late glacial or, in some places, interglacial origin. No tertiary deposits have been found in situ inside the valleys, but sequences interpreted as Oligocene clay and Miocene silt and sand are occasionally found among the Quaternary infill sediments (e.g. archive no. 45.533, 37.853, 45.418, GEUS 2003). These sequences have previously been interpreted as ice-rafted layers (Gravesen 1993; GEUS 2003), but when the borehole logs are combined with the TEM data, other interpretations become more likely. For instance, the low-resistive structure 4 (Figure 6, 8) seen in the TEM data between 20 m b.s.l. and 10 m a.s.l., is in several boreholes described as meltwater clay and clay till, but in some boreholes it is described as tertiary mica silt or clay (e.g. archive no. 45.418, GEUS 2003). It is likely that the micaceous sediments occurring in the Quaternary sequence consist of reworked tertiary material originating from the valley surroundings and re-deposited after valley incision. This implies that the usage of borehole logs alone may lead to erroneous interpretations when mapping buried valleys.

Viborg County has recently performed three deep exploration drillings in buried valleys on Mors (Krohn *et al.* 2004). The three drillings (archive no. 37.1241, 37.1242, 37.1248, GEUS 2003) are situated within the valley structures 1, 2 and 17. Except for some few metres of glaciomarine sediments around present-day sea level in one of the valleys (structure 1), all valley infill material is described as being glaciofluvial and glaciolacustrine sediments and till.

The widespread occurrence of lacustrine and marine clays in the valleys indicates that at least parts of the valleys were exposed during the following late or interglacial period.

Valley generations and relative ages. Multiple generations of buried Quaternary valleys are found in several parts of Denmark (Jørgensen *et al.* 2003a, 2003b; Sandersen & Jørgensen 2003; Jørgensen & Sandersen 2004) and adjoining areas (e.g. Salomonsen & Jensen 1994; Cameron *et al.* 1987; Wingfield 1989; Ehlers & Wingfield 1991; Piotrowski 1994; Praeg & Long 1997). As seen in the cross-sections (Fig. 8), more than one generation of buried valleys also seem to occur on Mors. Here, different valleys appear to incise each other (e.g. structures 1 and 1x; 4 and 6; 13 and 14; 11 and 12). Such multiple valley incisions can also be seen on the thematic maps, e.g. in the interval resistivity map of 40–50 m b.s.l. (Fig. 6), where two different parallel incisions can be seen within structure 1 just southeast of the dome structure. The eastern part of structure 1 contains sediments with high resistivities, whereas the western part contains sediments of low resistivity. This shows that a younger valley is cut into an older valley containing clayey sediments (the low resistivities) and subsequently filled with sandy sediments (the high resistivities).

Another example can be seen where the valley of structure 5 crosses structure 1. Here, low-resistive deposits extend across the valley of structure 1 indicating that it is cross-cut by structure 5 (dashed lines in Figure 6B, 40–50 m b.s.l.).

The cross-cutting character of the valleys shows that the buried valleys were not formed simultaneously and that several generations of valleys exist. Further indications on different valley generations occur where young buried valleys confined to the shallow part of the subsurface overlie older, deep-seated valleys. In such instances, infill deposits of young valleys can be detected in higher levels of the TEM-survey, independently of the deeper lying valley deposits. The most convincing example demonstrated in the thematic maps is where the valley of structure 4, which contains low-to-medium resistive layers, lies above the buried valleys of structures 1, 5, 6 and 7 (Fig. 6).

Sandersen & Jørgensen (2003) and Jørgensen & Sandersen (2004) distinguished multiple valley generations in various places in Denmark on the basis of preferred valley orientations and cross-cutting relationships. The orientations of the buried valleys on Mors appear to cluster within the three intervals: N–S to NNE–SSW, ESE–WNW to SSE–NNW and E–W to ENE–WSW, in the following referred to as: N–S, SE–NW and E–W respectively. It is proposed that these preferred orientations represent individual valley generations formed by multiple glaciations.

The proposed valley generations are outlined in Figure 9. All buried valleys found in the combined examination of TEM and borehole data are divided into different valley generations. The N–S orientation can additionally be divided into at least two separate generations located at different vertical levels and stratigraphic positions. A subdivision of the N–S oriented valleys is consistent with the fact that the valley of structure 4 is younger than structure 1, although they are almost parallel to each other. The occurrence of more than one N–S generation is also evident at several other places on the island, but not shown by figures presented here. Furthermore, the sound between Mors and Salling southeast of Mors occupies an open valley. Since this valley has not been buried during later events, it may belong to a young N–S generation, most likely younger than its buried counterparts. Several N–S oriented generations of valleys therefore seem to exist, but here it has only been possible to define two separate generations of N–S oriented buried valleys (Fig. 9).

Apart from the relationship between the two N–S generations, the age relation between the four valley generations is difficult to determine precisely. Indications of the age relations occur where valleys with
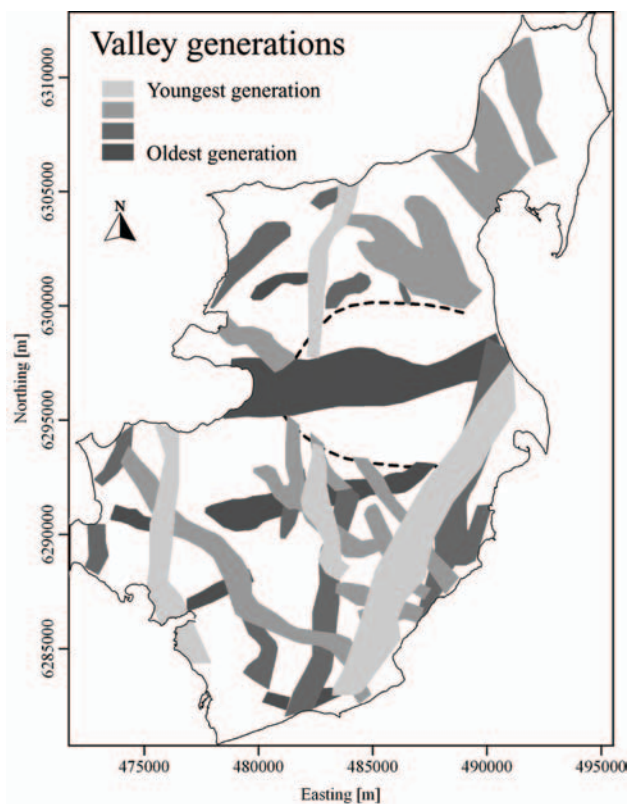

Fig. 9. Map of all the identified buried valleys divided into four proposed valley generations of different ages. Age relationships are indicated, and the location of the salt diapir is marked with a broken line. Scale: 5 km between axis ticks. Coordinate system: UTM zone 32/ED50.

contrasting infill resistivities crosscut each other. All indications of age relations like this have been examined and compared for the entire island (Fig. 9). The E–W generation is most likely older than the two N–S generations, and the SE–NW generation is found to be younger than the first N–S generation, but older than the second one.

Sedimentological analyses of borehole samples from the three deep exploration drillings (archive no. 37.1241, 37.1242, 37.1248, GEUS 2003) performed by Viborg County indicate that the infill deposits in three valleys (structures 1, 2 and 17) are of Saalian and Weichselian age, and it is therefore proposed that the three valleys were formed during the Saalian glaciation or earlier (Krohn et al. 2004).

Interglacial marine clay found in two boreholes in the central southern part of the island (archive no. 37.771 and 37.775, GEUS 2003; Gravesen 1993) appears to represent infill sediments in a N–S oriented buried valley. The valley occurs as a distinct low-resistive elongate body on the interval resistivity maps of 10 to 30 m a.s.l. (not presented in the figures), and the marine clay was found in the bore-

holes between 20,5 and 32,5 m a.s.l., corresponding to the low-resistive layer in the TEM soundings. For marine interglacial sediments, such high positions above present day sea level are rather unexpected, but the correlation between the marine clay in the boreholes and the layer in the TEM models indicates that the clay has not been disturbed. The layer can be followed for about 4 km along and about 1 km across the valley. Other occurrences of marine clay situated at the same high elevations above sea level have been found just south of Mors at the Hostrup locality (Ussing 1903; Knudsen 1977). This clay (the Hostrup Clay) was supposed to be of Late Elsterian–Holsteinian age and was found between 20 and 26 m a.s.l. It is, however, unclear whether the Hostrup Clay is disturbed or not, but its relatively widespread distribution in the area indicates that it has retained its original position. Foraminiferal assemblages in the marine clay in the boreholes on Mors point to a Late Elsterian–Early Holsteinian age (Peter Konradi, personal communication 2004), and since this valley is a member of the youngest valley generation, all generations (Fig. 9) may be of Elsterian age or older. This interpretation is based on foraminifera biostratigraphy and correlation between the marine clay and the low-resistive layer in the TEM soundings and is therefore tentative.

The subglacial valleys observed in the present day landscape and the Saalian and Weichselian sediments found within some of the buried valleys (Krohn *et al.* 2004) perhaps reflect formation of some of the valleys during these glaciations.

Glaciotectonic thrust complexes

Glaciotectonic structures in the TEM survey. The glaciotectonic complex at Hanklit in the northern part of Mors is clearly expressed in the terrain as imaged in Figure 2. Black polygons outline the areas in which ice-shoved hills and ridges occur in composite-ridge systems in the Hanklit area (partly after Klint & Pedersen 1995). The same areas are superimposed onto the map of the low-resistive layer (Fig. 5) and on the interval resistivity slices (Fig. 6).

In general, the low-resistive layer and the morphology of the glaciotectonic complex correlate (Fig. 5). Especially in the northern parts of the two large composite-ridge system areas, the low-resistive layer is elevated to high positions (to about 60 m a.s.l.) and almost exposed at the surface. Elsewhere, for instance where buried valleys incise the low-resistive layer, or below the two smaller areas to the north, the surface of the low-resistive layer does not correlate with the surface topography.

The morphology of the low-resistive layer is also indicated in the interval resistivity maps (Fig. 6). In this figure it appears that most of the composite-ridge systems are composed of layers with resistivities below 10 ohm-m, but some parts show low-to-intermediate resistivities or even high resistivities. The glaciotectonic complex can be traced as low-resistive structures in the TEM maps to a depth of about 30 m b.s.l. It is not present in the slice of 40–50 m b.s.l. and below since no resistivity contrasts between the complexes and the surrounding layers occur here.

The glaciotectonic complexes on the far northeastern part of Mors are also shown on Figure 2, 5 and 6 (after Gry 1979). Grey lines here mark the distal front of the complexes which in the terrain primarily occur as small ice-shoved ridges. The glaciotectonic features are less distinct than the Hanklit glaciotectonic complex, but some of them are well expressed in the terrain (Fig. 2). Correlation between the ice-shoved ridges seen in the terrain and the results of the TEM survey is evident (Figs 5, 6). Ridge-like structures of low resistivity occur on the eastern margin of the grey lines corresponding to the core of the complexes. They seem to terminate abruptly at the grey lines and can be traced as deep as around 50 m b.s.l. The westernmost ice-marginal moraine is denoted with an 'M' on the cross-section (Fig. 8B). Only a small ridge is seen in the terrain here.

Due to sparse data coverage in the far northeastern part of the island the Ejerslev glaciotectonic complex (Pedersen 2000) is not revealed by the TEM survey.

Lithology of the glaciotectonic structures. Borehole logs from drillings (Gravesen 1990; GEUS 2003) located in the composite-ridge systems of the Hanklit area show that the low-resistive layers elevated to high positions mainly correspond to Oligocene clays (e.g. archive no. 37.760, 37. 816, 37.850, GEUS 2003). Some borehole logs in the ridge systems show thick successions of glacial sediments (e.g. archive no. 30.949, 37.617, 37.1049, GEUS 2003), but these are situated in places where high resistivities dominate the succession or where the TEM data density is low. The majority of boreholes in the low-lying areas between the ridge systems or immediately outside the ridge systems show glacial deposits in the upper part of the succession. Deep boreholes in these areas show diatomite and other Paleogene sediments at greater depths.

Extensive occurrences of diatomite are exposed in cliffs and pits along the proximal (northern) parts of the Hanklit glaciotectonic complex (Klint & Pedersen 1995). At Hanklit cliff these layers are intensely folded and thrusted in several thrust sheets that also

involve glacial sediments. The Paleogene diatomite is also evident in borehole logs. It occurs within a margin of around 1 km along the coast, including the two small ridge systems to the north and the northern part of the large easternmost system. In the thematic maps (Figs 5 and 6) it appears that the TEM soundings mainly show low-to-moderate resistivities (10–40 ohm-m) to depths of about 20 m b.s.l in the diatomite-dominated margin along the coast. This is in accordance with the expected resistivity values for the diatomaceous sediments. A cross-section through the complex is presented in Figure 8C (see Figs 4, 5 and 6 for location). The structure 16-valley is seen in the southern part of the section and the coast is situated in the northern part. Sediments (thrust sheets) of low resistivities corresponding to Paleogene clay (Oligocene) are elevated to high positions in the middle part of the section ('pc') whereas sediments with somewhat higher resistivities (light bluish colours) corresponding to diatomite ('ed') occur in the northern part.

As described above, the cores of the composite-ridge systems at Hanklit contain a variety of sediment types. The combined TEM and borehole data indicate that thrust sheets consisting of diatomite have been transported into the proximal parts of the complex and thrust sheets of Oligocene clay into the middle or distal parts (Fig. 8C). This distribution of thrust sheets inside the glaciotectonic complex may reflect that the distal part was formed before the proximal part: Thrust sheets from the upper part of the succession in the source area were displaced first (distally) before older, deeper layers were displaced proximally in the glaciotectonic complex. Large parts of the systems are also occupied by high-resistive glacial deposits. These deposits may be incorporated in thrust sheets, but in the deeper part of the succession the glacial sediments seem to be related to buried valley structures, as discussed below.

According to borehole logs, the glaciotectonic complexes in the northeastern part of Mors are also partly dominated by diatomite in narrow zones. The diatomite corresponds to layers with low-to-medium resistivities in the TEM soundings and is shown with light bluish colours in the interval resistivity maps from around sea level to somewhere between 30 and 50 m b.s.l (Fig. 6). Resistivities less than 10 ohm-m below this level indicate a dominance of Paleogene clay ('pc') below the diatomite; however no borehole information is available at this depth. The cross-section in Figure 8B illustrates this situation with layers with low resistivities gradually dominating the succession downwards (from 4000 to 5500 m and from 7000 to 7500 m). Borehole logs and the TEM survey show that the uppermost part of the succession

(above sea level) in the area consists of various sediments. Layers with medium resistivities occur between ground level and sea level underneath the ice-marginal moraine 'M' in the cross-section. This corresponds to the sequence of various deposits described by Korsager (2002) at Skærbæk Klint, situated where the coastline crosses the ice-marginal moraine close to the cross-section. Folded and thrusted layers of mainly diatomite and glacial deposits are exposed here.

Relationships between the individual geological elements

Buried valleys and glaciotectonic thrust complexes. Some of the buried valleys can be followed below the glaciotectonic complex at Hanklit (Figs 5, 6). The buried valley described as structure 15 extends below the northeastern part of the complex as seen in the interval resistivity map of 40 to 50 m b.s.l. and in the surface of the low-resistive layer. The valley of structure 16 can be followed into the western part of the complex from approximately 10 m a.s.l. down to about 60 m b.s.l. This valley terminates towards the northeast where the complex is composed of Paleogene clay; these clays have very low resistivities and are difficult to penetrate with the TEM method. As a consequence, the depth of penetration through this clay is likely to be less than 50 m, and it is therefore possible that the valley extends all the way underneath the glaciotectonic complex. A short valley segment occurring in the low-resistive layer northeast of the clay ridge (Fig. 5) may therefore be interpreted as the extension of the structure 16-valley on the other side of the complex. It is obvious that the structure 16-valley was present before thrusting of the ridge system, and that the valley structure was heavily disturbed by thrust sheets of Paleogene clay.

Northwards the buried valley of structure 17 can be followed to the coast between the two large areas of composite-ridge systems (Figs 5, 6). The northern part of the valley is filled with deposits with fairly low resistivities and therefore hardly visible in the interval resistivity maps due to the low contrasts. However, this part of the valley can be seen in the surface of the low-resistive layer. The southern part is filled with deposits with various resistivities, corresponding to glacial deposits, as also described in one of the three exploratory drillings (archive no. 37.1242, GEUS 2003) on Mors by Krohn *et al.* (2004). The following observation indicates that this valley is also older than the deformations: The buried valley seems to be wider than the overlying topograph-

ical valley situated between the two composite-ridge system areas. This can particularly be observed where the valley in the landscape is narrow and crosses a distinct threshold (compare Figs 2, 5 & 6). The formation of the buried valley of structure 17 and the glaciotectonic complex can be interpreted as follows: A valley was subglacially eroded and was left by the glacier, open or buried, in the area before the glaciotectonic events took place. Paleogene clay and diatomite, together with glacial sediments, were folded and thrusted, and the composite-ridge systems were formed. Parts of the valley became glaciotectonically disturbed, and the fill sediments, as well as the surrounding layers, were thrusted into the glaciotectonic complex. The smaller valley occurring in the landscape above the buried valley is interpreted as a tunnel valley leading meltwater through the composite-ridge systems to an ice front situated at the topographic threshold (Andersen & Sjørring 1992). The meltwater that eroded the tunnel valley probably found its way to the ice front by reusing the pathway of the older buried valley, as seen elsewhere on Mors (e.g. structure 1) and in other parts of Denmark and adjoining areas where multiple valley incisions occur within larger valley structures (e.g. Piotrowski 1994; Dobracki & Krzyszkowski 1997; Sandersen & Jørgensen 2003; Jørgensen & Sandersen 2004). The buried valley was therefore formed ahead of the Weichselian Main Advance, which is believed to have covered the area after the glaciotectonic deformations took place (e.g. Gry 1979; Ditlefsen 1991; Pedersen 1996; Korsager 2002). This is also in accord with borehole sample analyses from the exploratory drilling, which indicated that the valley infill was from Early Weichselian and/or the Saalian glaciations (Krohn *et al*. 2004).

In the northeastern part of Mors the buried valleys are oriented parallel to the glaciotectonic structures. The TEM data contain no direct evidence for an age relationship between the buried valleys and the glaciotectonic structures here. However, based on lithostratigraphic investigations carried out by Korsager (2002), it can be concluded that these valleys are also older than the phase of glaciotectonic deformation, because the Hanklit Till, which is incorporated in the glaciotectonic structures at Skærbæk Klint, is found relatively undisturbed in the uppermost covering sequence of the buried valleys (structures 11 and 12) situated immediately southwest of Skærbæk Klint.

Consequently, the valleys must have been present as buried or open features prior to the glaciotectonic events, and the location of the ice-marginal moraines along the northeastern edges of the valleys on the northeastern part of the island indicates that the val-

leys may have affected the processes of glaciotectonic activity. The glaciotectonic décollement horizons in the area have been estimated to be present within the clayey Holmehus Formation below the Fur Formation at a level of around 50 m b.s.l. at Skærbæk Klint (Korsager 2002) and around 80–100 m b.s.l. at Feggeklit (Pedersen 1996). The valleys of structures 11 and 13 reach depths of more than 70 m b.s.l. and the valleys are therefore deeper than the estimated depth of the décollement horizon at Skærbæk Klint which is situated between the valleys. If the development of décollement horizons in the area is dependent on the lithology as argued by Pedersen (1996) and Korsager (2002), the glaciotectonic deformation will tend to occur outside the valleys where the Holmehus Formation is present.

Structures 13 and 14 occur as elongate depressions containing sediments with high resistivities and are interpreted as subglacial valleys, but it cannot be excluded that the structures could be source depressions for the thrust complex and subsequently filled with glacial sediments during the ice advance or retreat. Nevertheless, glaciotectonic source depressions do not normally occur as elongate valley-like structures like those appearing in the TEM survey, but the buried valleys may have been partly deformed by subsequent glaciotectonic activity. It is very likely that the valley flanks facing east and northeast are strongly influenced by the glaciotectonic deformations.

Formation of the glaciotectonic complexes on Mors seems to have been affected by the presence of buried valleys. This may have happened either as a response to the valley topography or because the décollement horizon is absent in the buried valleys due to deep erosion. It is thus presumed that the pre-existing valleys have had significant local impact on the glaciotectonic events.

Glaciotectonic thrust complexes and the salt diapir. As already pointed out by other authors, there seems to be a close relationship between the location of the glaciotectonic complexes and the salt diapirs and domes in the area (e.g. Gry 1979; Pedersen 2000; Klint & Pedersen 1995). The development of glaciotectonic activity is strongly dependent on the presence of clayey Paleogene deposits, and the absence of these layers above the salt diapir prevents the formation of glaciotectonic complexes. Diapir flanks dipping against the ice movement direction are also able to initiate formation of glaciotectonic complexes (Pedersen 2000).

Buried valleys and the salt diapir. Despite some difficulties in achieving exact images of the buried valleys when they cross the salt diapir, it is demonstrat-

ed that several buried valleys incise its covering layers. The formation of most of these valleys seem to be relatively unaffected by the presence of the diapir. An exception, however, is the E-W oriented buried valley incised in the relatively soft chalk between the more consolidated Danian limestones (structure 3) which indicates some kind of correlation to the substratum. The location, and probably also the formation, of this valley is apparently controlled by the contrasts in the erodibility of the substrate, by faults or by a graben structure created by extension above the salt diapir. Relationships between deep-seated structural elements and buried valleys in Denmark have been described and documented by Jørgensen & Sandersen (2004). They demonstrate that deep-seated faults, possibly reactivated by postglacial rebound, to some extent tend to control the location and orientation of subglacial valley erosion.

Conclusions

Detailed examination of the TEM data from Mors shows that large-scale TEM surveys are able to improve the geological understanding of the regional geological setting to a depth of around 150 meters. TEM surveys add important new and detailed information about the spatial distribution of geological structures, and make a valuable contribution to the geological model.

Improvements in TEM instrumentation, data processing, data handling and data presentation over the past few years have made the TEM method a powerful tool in geological field mapping. In addition to this, increasing practical experience with geological interpretation of TEM data has improved its contribution to geological models. The TEM method offers excellent images of deep-seated low-resistive layers, such as the Paleogene clay, and is capable of resolving geological structures and layers in the overlying succession.

Geological structures are delineated by assessing resistivity distributions from surface and interval resistivity maps, whereas the lithology is assessed from the measured resistivity values. In this way both structural and lithological information is acquired from the same data set, thus adding important information for interpretation of the geological environment.

The TEM survey on Mors shows that, due to the complex geological succession, borehole logs cannot constitute the basis for the geological interpretation alone, although the density of boreholes is relatively large.

Apart from facies variations the complicated geology found on Mors is primarily a result of three processes: 1) deformation by halokinesis, 2) erosion of valleys and 3) glaciotectonic thrusting. The morphology of the layers over the Mors salt diapir is clearly demonstrated by the TEM survey as an ellipsoid-shaped structure. Paleogene clay rests upon Danian limestone which partly covers the Maastrichtian chalk. Saline pore water is present in the chalk 50–80 m b.s.l. Numerous buried valleys dissect the entire island, including the layers over the salt diapir. The valleys are widespread and can be divided into different generations, each having their own preferred orientation. In places where they overlie or cross each other, the relative ages of valley generations can be estimated. Four generations have been identified, but more may exist. Most of the valleys are presumed to be old, most likely formed during the Elsterian glaciation or earlier. The buried valleys are mainly filled with glacial sediments, but interglacial sediments also occur. Many valleys contain lacustrine and marine clays in their upper parts up to levels between sea level and 30 m a.s.l. The large glaciotectonic complexes on Mors are also exposed in the TEM survey. The central parts of the Hanklit glaciotectonic complex are primarily composed of thrust sheets of Paleogene clay, whereas thrust sheets and folds containing diatomite are found in the proximal parts. This indicates that the distal and central parts of the complexes were formed prior to the proximal parts. The survey also shows that the glaciotectonic complexes are young features, formed after the buried valleys, and it is likely that the buried valleys had a considerable effect on the formation of the glaciotectonic complexes.

Acknowledgements

References

Aber, J.S., Croot, D.G. & Fenton, M.M. 1989: Glaciotectonic land-forms and structures. 200 pp. Glaciology and Quaternary Geology Series, Kluwer Academic Publishers, Dordrecht, the Netherlands.

Andersen, S. & Sjørring, S. 1992: Geologisk Set. Det nordlige Jylland. En beskrivelse af områder af national geologisk interesse. 208 pp. Geografforlaget.

Auken, E. & Christiansen, A.V. 2004: Layered and laterally constrained 2D inversion of resistivity data. Geophysics 69, 752–761.

Auken, E., Jørgensen, F. & Sørensen, K. 2003: Large-scale TEM investigation for groundwater. Exploration Geophysics 34, 188–194.

Auken, E., Christiansen, A.V., Jacobsen, L. & Sørensen, K.I. 2004: Laterally Constrained 1D-Inversion of 3D TEM Data. A8, 4 pp. EEGS-NS. Extended Abstracts Book. 10th meeting EEGS-NS, Utrecht, The Netherlands.

Cameron, T.D.J., Stoker, M.S. & Long, D. 1987: The history of Quaternary sedimentation in the UK sector of the North Sea Basin. Journal of the Geological Society London, 144, 43–58.

Christensen, N.B. & Sørensen, K.I., 1998: Surface and borehole electric and electromagnetic methods for hydrogeological investigations. European Journal of Environmental and Engineering Geophysics, 75–90.

Danielsen, J.E., Auken, E., Jørgensen, F., Søndergaard, V. & Sørensen, K. 2003: The application of TEM in hydrogeophysical surveys. Journal of Applied Geophysics 53, 181–198.

Dansk Geofysik 2002: Geofysisk kortlægning på Mors. Transiente elektromagnetiske (TEM) sonderinger. July 2002. 14 pp.

Ditlefsen, C. 1991: Luminiscence Dating of Danish Quaternary Sediments. 116 pp. Unpublished PhD thesis. Institute of Earth Sciences, Aarhus University, Aarhus, Denmark.

Dobracki, R. & Krzyszkowski, D. 1997: Sedimentation and erosion at the Weichselian ice-marginal zone near Golczewo, northwestern Poland. Quaternary Science Reviews 16, 721–740.

Effersø, F., Auken, E., & Sørensen, K.I. 1999: Inversion of band-limited TEM responses. Geophysical Prospecting 47, 551–564.

Ehlers, J. & Wingfield, R. 1991: The extension of the Late Weichselian/Late Devensian ice sheets in the North Sea Basin. Journal of Quaternary Science 6, 313–326.

Elkraft & Elsam 1981: Disposal of high-level waste from nuclear power plants in Denmark. Salt dome investigations. 411 pp. Elsam and Elkraft, report, June 1981. Volume II, Geology.

Fitterman, D.V. & Stewart, M.T. 1986: Transient electromagnetic sounding for groundwater. Geophysics 51, 995–1005.

Fitterman D.V., Meekers, J.A. & Ritsema, I.L. 1988: Equivalence behavior of three electrical sounding methods as applied to hydrogeophysical problems. Proceedings of the 50th Annual Meeting and Technical Exhibition of the European Association of Exploration Geophysicist, p. 37.

Fountain, D. 1998: Airborne Electromagnetic System - 50 years of development: Exploration Geophysics 29, 1–11.

GeoFysikSamarbejdet 2003: Anvendelse af TEM-metoden ved geologisk kortlægning. GeoFysikSamarbejdet. Århus Universitet. 72 pp. [http://www.gfs.au.dk]

GEUS 2003: The national well data archive. Viborg Amt. [www.geus.dk/jupiter]

Goldman, M., Tabarovsky, L. & Rabinovich, M. 1994: On the influence of 3-D structures in the interpretation of transient electromagnetic sounding data. Geophysics 59, 889–901.

Gravesen, P. 1990: Geological map of Denmark 1:50.000. Kortbladet 1116 I Thisted. Geologisk basisdatakort. Geological Survey of Denmark. Map series no. 13.

Gravesen, P. 1993: Geological map of Denmark 1:50.000. Kortbladet 1116 II Nykøbing Mors. Geological basic data map. Geology of Denmark Map Series 21.

Gry, H. 1940: De istektoniske Forhold i Moleret. Meddelelser fra Dansk Geologisk Forening 9, 586–627.

Gry, H. 1979: Beskrivelse til Geologisk Kort over Danmark, kortbladet Løgstør. Danmarks Geologiske Undersøgelse, I. Række 26, 58 pp. + atlas + map. Vol. (with summary in English).

Houmark-Nielsen, M. 1999: A lithostratigraphy of Weichselian glacial and interstadial deposits in Denmark. Bulletin of the Geological Society of Denmark 46, 101–114.

Houmark-Nielsen, M. 2003: Signature and timing of the Kattegat Ice Stream: initiation of the LGM-sequence at the southwestern margin of the Scandinavian Ice Sheet. Boreas 32, 227–241.

Huuse, M. & Lykke-Andersen, H. 2000: Overdeepened Quaternary valleys in the eastern Danish North Sea: morphology and origin. Quaternary Science Reviews 19, 1233–1253.

HydroGeophysics Group, University of Aarhus (HGG) 2004a: Getting strated with SiTEM and Semdi. Manual. Web document: [http://www.hgg.au.dk].

HydroGeophysics Group, University of Aarhus (HGG) 2004b: SiTEM/Semdi processing and inversion package. Web document: [http://www.hgg.au.dk].

HydroGeophysics Group, University of Aarhus (HGG) 2004c: Manual for the inversion program em1dinv. Web document: [http://www.hgg.au.dk].

HydroGeophysics Group, University of Aarhus (HGG) 2004d: Workbench. Web document: [http://www.hgg.au.dk].

Japsen, P. & Bidstrup, T. 1999: Quantification of late Cenozoic erosion in Denmark based on sonic data and basin modelling. Bulletin of the Geological Society of Denmark 46, 79–99.

Jensen, J.B. 1985: Sen-Elster smeltevandsler - en mulig ledehorisont i det vestlige Jylland. Dansk Geologisk Forening, Årsskrift for 1984, 21–35.

Jørgensen, F. & Sandersen, P. 2004: Kortlægning af begravede dale i Jylland og på Fyn. Opdatering 2003–2004. 178 pp. De jysk-fynske amters grundvandssamarbejde. Vejle Amt, Watertech. [www.buried-valleys.dk].

Jørgensen, F., Lykke-Andersen, H., Sandersen, P.B.E., Auken, E. & Nørmark, E. 2003a: Geophysical investigations of buried valleys in Denmark: An integrated application of transient electromagnetic soundings, reflection seismic surveys and exploratory drillings. Journal of Applied Geophysics 53, 215–228.

Jørgensen, F., Sandersen, P.B.E & Auken E. 2003b: Imaging Buried Valleys using the Transient Electromagnetic Method. Journal of Applied Geophysics 53, 199–213.

Kjær, K.H., Houmark-Nielsen, M. & Richardt, N. 2003: Ice-flow patterns and dispersal of erratics at the southwestern margin of the last Scandinavian Ice Sheet: signature of paleo-ice streams. Boreas 32, 130–148.

Klint, K.E.S. & Pedersen, S.A.S. 1995: The Hanklit Glaciotectonic Thrust Fault Complex, Mors, Denmark. Danmarks Geologiske Undersøgelse, DGU Serie A 35, 30 pp.

Knudsen, K.L. 1977: Foraminiferal faunas of the Quaternary Hostrup Clay from northern Jutland, Denmark. Boreas 6, 229–245.

Korsager, B. 2002: En strukturel og sedimentologisk undersøgelse af klinten ved Skærbæk, Nord Mors. 95 pp. Unpublished M.Sc. thesis, University of Copenhagen, Denmark. [www.geologen.dk].

Krohn, C., Kronborg, C., Nielsen, O.B., Knudsen, K.L., Sørensen, J. & Kragelund, A. 2004: Boring DGU. Nr. 37.1241, 37.1242 og 37.1248. Report No. 04VB-01. 64 pp. University of Aarhus, Denmark.

Larsen, G. & Baumann, J. 1982: Træk af Mors salthorstens udvikling. DGF Årsskrift for 1981, 151–155.

Larsen, G. & Kronborg, C. 1994: Det mellemste Jylland. En beskrivelse af områder af national geologisk interesse. 272 pp. Geografforlaget.

Madirazza, I. 1977: Zechstein bassinet og saltstrukturer i Nordjylland med særligt henblik på Nøvling og Paarup. Dansk Geologisk Forening, Årsskrift for 1976, 57–68

McNeill, J.D. 1990: Use of electromagnetic methods for groundwater studies. In: Ward, S.H. (ed.): Geotechnical and Environmental Geophysics. Society of Exploration Geophysicists. Investigations in geophysics 5, 191–218.

Mills, T., Hoekstra, P., Blohm, M. & Evans, L. 1988: Time domain electromagnetic soundings for mapping sea-water intrusion in Monterey County, California. Ground Water 26, 771–782.

Newman, G.A., Hohmann, G.W. & Anderson, W.L. 1986: Transient electromagnetic response of a three-dimensional body in a layered earth. Geophysics 51, 1608–1627.

Pedersen, S.A.S. 1996. Progressive glaciotectonic deformation in Weichselian and Paleogene deposits at Feggeklit, northern Denmark. Bulletin of the Geological Society of Denmark 42, 153–174.

Pedersen, S.A.S. 2000: Superimposed deformation in glaciotectonics. Bulletin of the Geological Society of Denmark 46, 125–144.

Pedersen, G.K. & Surlyk, F. 1983: The Fur Formation, a late Paleocene ash-bearing diatomite from northern Denmark. Bulletin of the Geological Society of Denmark 32, 43–65.

Piotrowski, J.A. 1994: Tunnel-valley formation in northwest Germany - geology, mechanisms of formation and subglacial bed conditions for the Bornhöved tunnel valley. Sedimentary Geology 89, 107–141.

Poulsen, L. H. & Christensen, N. B. 1999: Hydrogeophysical mapping with the transient electromagnetic sounding method. European Journal of Environmental and Engineering Geophysics 3, 201–220.

Praeg, D. & Long, D. 1997: Buried sub- and proglacial channels: 3D-seismic morphostratigraphy. In: T. A. Davies, T. Bell, A. K. Cooper, H. Josenhans, L. Polyak, A. Solheim, M. S. Stoker & J. A. Stravers (eds): Glaciated continental margins: an atlas of acoustic images, 66–67. Chapman & Hall, London.

Salomonsen, I. & Jensen, K.A. 1994: Quaternary erosional surfaces in the Danish North Sea. Boreas 23, 244–253.

Sandersen, P.B.E. & Jørgensen, F. 2003: Buried Quaternary valleys in the western part of Denmark – occurrence and implications for groundwater resources and vulnerability. Journal of Applied Geophysics 53, 229–248.

Spies, B.R. 1989: Depth of investigation in electromagnetic sounding methods. Geophysics 54, 872–888.

Spies, B.R. & Frischknecht, F.C. 1991: Electromagnetic sounding. In: Nabighian, M.N. (ed.): Electromagnetic Methods in Applied Geophysics. Society of Exploration Geophysicists. Investigations in geophysics 2, 398–402.

Sørensen, K. I. and Auken, E. 2004: SkyTEM - A new high-resolution helicopter transient electromagnetic system. Exploration Geophysics 35, 191–199.

Sørensen, K.I., Effersø, F. & Auken, E. 2001a: A hydrogeophysical Investigation of the Island of Drejø. European Journal of Environmental and Engineering Geophysics 6, 109–124.

Sørensen, K.I., Thomsen, P., Auken, E. & Pellerin, L. 2001b: The effect of Coupling in Electromagnetic Data, 108–109. EEGS. Proceedings - Electrical and Electromagnetic Methods Session (ELEM). Birmingham, England.

Sørensen, K.I., Auken, E., Christensen, N.B. & Pellerin, L. in press: An Integrated Approach for Hydrogeophysical Investigations: New Technologies and a Case History. Near Surface Geophysics II: Applications and Case Histories, Society of Exploration Geophysicists.

Sørensen, K.I., Sørensen, B., Christiansen, A.V. & Auken, E. 2004b: Interpretation of a Hydrogeophysical Survey - Data from the High-resolution SkyTEM System. 10th meeting EEGS-NS, Utrecht, The Netherlands.

Ussing, N.V. 1903: Om et nyt findested for et marint Diluvium ved Hostrup i Salling. Naturhistorisk Forening 1903, 111–123. Kjøbenhavn.

Wingfield, R. 1989: Glacial incisions indicating Middle and Upper Pleistocene ice limits off Britain. Terra Nova 1, 538–548.